Applied Catalysis B: Environmental 221 (2018) 530–555

Contents lists available at ScienceDirect

Applied Catalysis B: Environmental

journal homepage: www.elsevier.com/locate/apcatb

Review

Current status, opportunities and challenges in catalytic and photocatalytic applications of aerogels: Environmental protection aspects

Hajar Maleki*, Nicola Hüsing*

Institute of Materials Chemistry, Paris-Lodron University Salzburg, Jakob-Haringer-Strasse 2a, 5020 Salzburg, Austria

ARTICLE INFO

Article history:
Received 15 May 2017
Received in revised form 22 July 2017
Accepted 2 August 2017
Available online 25 August 2017

Keywords:
Aerogel catalyst
Aerogel photocatalyst
Environmental remediation
Air cleaning
Water cleaning

ABSTRACT

Aerogels are an exceptional class of materials which are of interest for several high-performance applications thanks to their extraordinary physical properties such as extremely high porosity, high specific surface area, and extremely low density combined with very versatile synthesis approaches. Since their invention by S. Kistler, various aerogels have been explored for catalytic and photocatalytic applications, though in the recent decades, several breakthroughs regarding different aspects ranging from more efficient catalysis in organic synthesis, energy-related processes, and catalytic environmental depollution by aerogels have been made. For both, catalytic and photocatalytic performances, aerogel monoliths prepared from sol–gel approaches accompanied with an appropriate drying technique, in particular supercritical point drying, have become striking alternative catalysts or catalyst supports compared to the presently used ones prepared from traditional wet synthesis approaches. In this article, aerogels in environmental remediation processes as heterogeneous catalyst and photocatalyst for depollution of air and aqueous media are fully addressed, and recent achievement in this context is thoroughly reviewed.

Contents

* Corresponding authors.
E-mail addresses: hajar.maleki@sbg.ac.at (H. Maleki), nicola.huesing@sbg.ac.at (N. Hüsing).

http://dx.doi.org/10.1016/j.apcatb.2017.08.012
0926-3373/

1. Introduction

Aerogels are sol–gel derived porous materials with extraordinary properties, such as a high porosity, extremely low density, enormous active surface area and very low thermal conductivity [1]. The unique properties of aerogels originate from the combination of the specific properties of nanomaterials magnified by their macroscale assembly making aerogels attractive materials for several applications ranging from thermal and acoustic insulation, and catalysis to biomedical and pharmaceutical applications [2–4]. Among high-performance applications, *e.g.* as thermal insulators [4,5], aerogels have been recognized as catalysts or catalyst supports in various reactions [6,7].

Historically, the first aerogels were introduced by Kistler in the 1930s [8] by applying the supercritical drying method for the first time. However, in the following years, due to the progress in precursor chemistry and drying methods, various aerogels having organic as well as inorganic or even hybrid building blocks emerged [9]. Basically, irrespective of the building blocks and components, aerogels refer to solid materials having a three-dimensional porous network with interconnected micro/mesopores obtained by drying technologies that are able to conserve the initial wet gel structure [1].

Following the major interest of chemical industry in designing innovative materials as a solid catalyst, in recent years, major interest has been given to tailor-made aerogels as heterogeneous catalysts or catalyst supports for various reactions. In fact, Kistler [10] was a pioneer to recognize the catalytic applications of aerogels which were later pursued by several scientists, mainly Teichner, Baiker, Pajonk, and other groups [11–16]. In the 1990s, a series of reviews addressing the different gas and liquid phase catalytic aspects of aerogels particularly with the prospect of environmental protections were published by the same scientists [6,7]. So far, aerogels and their composites have been employed in both liquid–solid, and gas–solid catalyzed reactions in several domains, such as environmental protection, organic synthesis including partial oxidation, epoxidation, nitroxidation, hydrogenation [16,17] as well as energy-related applications [14,15,18–20]. Aerogels were also considered as solid biocatalysts for specific biochemical syntheses or as an active component of biosensors [21–24].

Since the support is playing a pivotal role in catalysts design, the use of materials with deliberately tailored properties is highly desirable. The suitability of aerogels as a catalyst support is related to their fascinating textural and structural properties in combination with the versatility of the synthesis route, *e.g.* the sol–gel technique, which gives flexibility of controlling the texture, composition, homogeneity and structural features of solids from a molecular level [12,16,20]. Additionally, the sol–gel technique opens up new possibilities to tailor the materials properties through the addition of different components, *i.e.* dispersion of the various oxides or metals in an aerogel matrix, to design and tailor the chemistry of aerogel toward the particular catalytic reactions [20].

Catalysts are essential components for the treatment of air and water pollutants on the way to a sustainable and clean environment [25]. Aerogels from various molecular precursors are recognized as active heterogeneous catalysts for several catalytic and photocatalytic environmental remediation purposes [6,26,27].

To preserve the air quality, control of the emission of hazardous volatile organic compounds (VOCs), nitrogen oxides (NOx; NO, NO_2, N_2O, *etc.*), carbon monoxide (CO), greenhouse gases *i.e.* methane (CH_4) and carbon dioxide (CO_2), *etc.* being released from transportation, municipal and industrial sectors and combustion is necessary.

Nitrogen oxides, NOx gases are generated from the reaction of nitrogen, oxygen, and hydrocarbons at high temperatures. The primary sources of NOx emission are traffic, industry, refineries and power plants [28,29]. Catalytic conversion of NOx into less harmful gases, such as N_2 and H_2O, is quite a matured field, and several review papers exist covering this topic [30–32]. The selective catalytic reduction (SCR) of NOx with various reductants such as NH_3, hydrocarbons, CO and soot particles over various catalysts and catalyst supports are reported for NOx abatement, so far [33]. However, ammonia or aqueous solutions of ammonia have been the main reductants used in the selective reduction of NOx, especially in the gas turbines, power plants, and waste incinerators [33]. In this contribution, we specifically focus on the SCR of NOx using NH_3 as a reductant by exploiting vanadium supported various metal oxides or carbon aerogel catalysts.

Aerogels are also recognized as suitable candidates for the adsorption/absorption as well as catalytic combustion of VOC vapors from effluents due to their tunable textural *e.g.* high specific surface area and porosity and structural properties *e.g.* density and monolithic structures as well as tunable surface chemistry [34]. In this paper, combustion catalysis of various VOCs using noble metal catalysts such as Pt, Pd, *etc.* supported carbon aerogels and transition metal oxides are studied [26].

Aerogels are also attractive for CO removal from an enriched hydrogen stream which is produced on board vehicles through different reforming and fuel oxidation processes [127] – hydrogen being an ideal fuel for proton-exchange membrane fuel cells (PEMFC). The PEMFC has drawn significant attention due to its low operation temperature, high efficiency, high power density and its environmentally benign exhaust gases [126]. However, during hydrogen production, a significant amount of CO is produced that causes a serious poisoning of the anode catalyst (*e.g.* platinum or palladium) of the PEMFC. Therefore, it is necessary to remove CO from the hydrogen stream with a minimum loss of hydrogen [128]. So far, several strategies for CO removal have been proposed [122], among them the preferential oxidation of CO (CO-PROX) as the most effective catalytic process [129,130]. In this regard, inorganic aerogels based on noble metals as well as various bimetallic compounds supported on inorganic aerogels have shown better promises for CO-PROX compared to the conventional catalysts.

Aerogel contribution for methane reforming with CO_2 is also discussed from the perspective of environmental protection aspects, even though this process is more known for the production of clean H_2 energy and synthesis gases (CO/H_2) as a feedstock for Fischer–Tropsch synthesis of hydrocarbons. Noble metals, transition metals, and their bi-metallic doped metal oxide aerogels have been exploited to catalyze the methane reforming process. Beside catalyst preparation methods, structural parameters, coke resistivity and operational conditions like the type of the reactor are extremely influential in the efficiency of the process that would be elaborated in this review paper.

Photocatalyst technology using semiconductors, mainly TiO_2 or TiO_2 based composites, is another effective way to deal with the problems concerning pollution abatement in gaseous environments [35]. The ease of implementation in commercial settings as well as low energy requirement that uses the sun or artificial light as energy sources and the applicability to a wide range of indoor and outdoor pollutants (*i.e.* NOx, VOC, bacteria, airborne particles, *etc.*) make this process an attractive choice in the degradation of contaminants [36,37]. However, traditional methods of sample preparation for photocatalytic reactions using powder form samples are not efficient enough with respect to catalyst regeneration, and consequently, from an economic and recycling standpoint [38]. Studies have shown that the preparation of photocatalysts in a certain geometry with the high active surface area for instance in two – (*e.g.* films) or three-dimensional structures (*e.g.* aerogels) for loading of the large amount of photoactive phases without any loss in catalyst during the process is becoming a compelling and critical

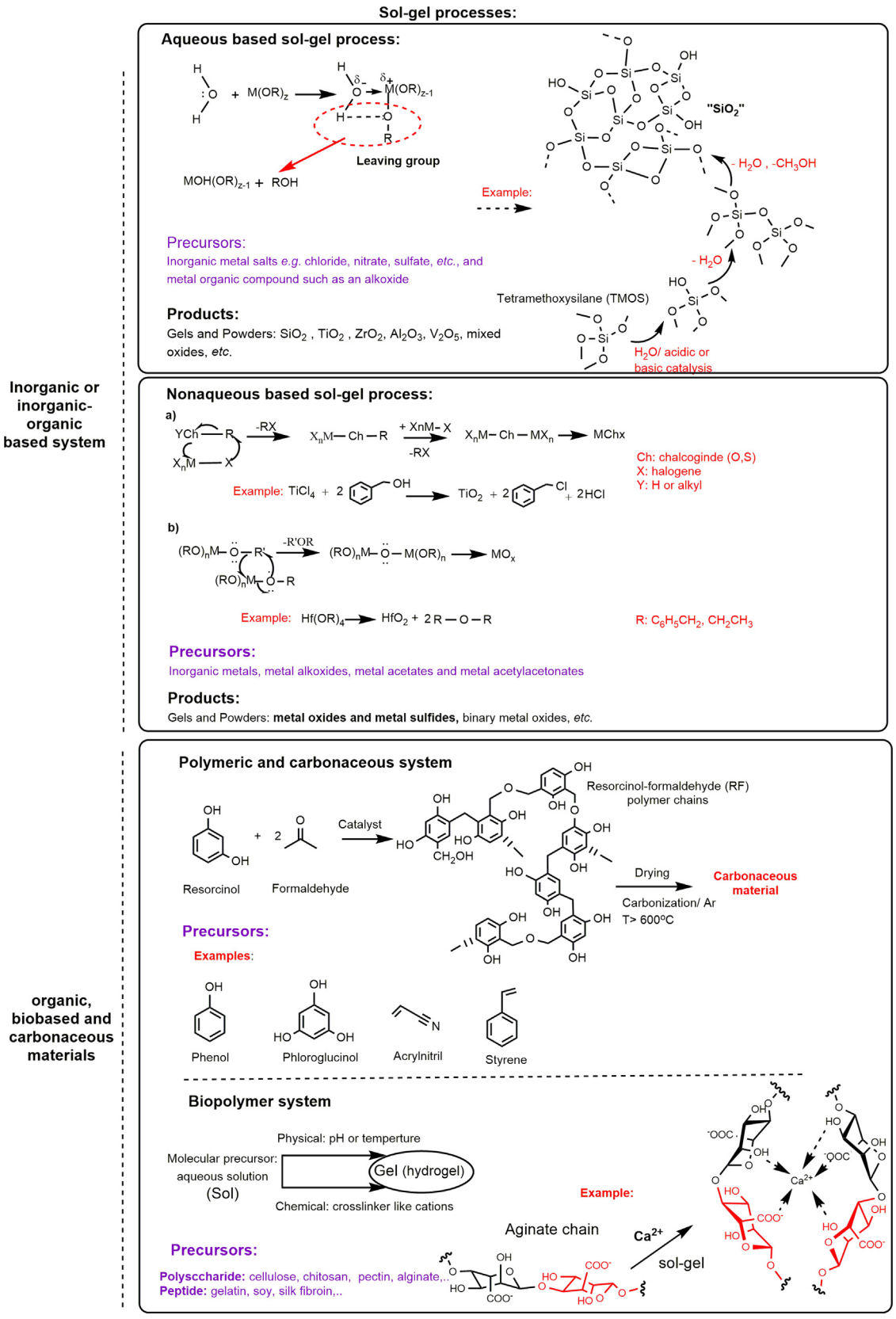

Fig. 1. Schematic description of the sol–gel process.

issue [38,39]. Photoactive aerogels like TiO_2 and TiO_2 supported silica or other oxides aerogels are being actively explored for air pollutant capturing and photodecomposition.

Another major threat to the environment and human health relies on water pollution, as wastewaters contain a wide variety of pollutants including dyes or other complex organics, eutrophi-

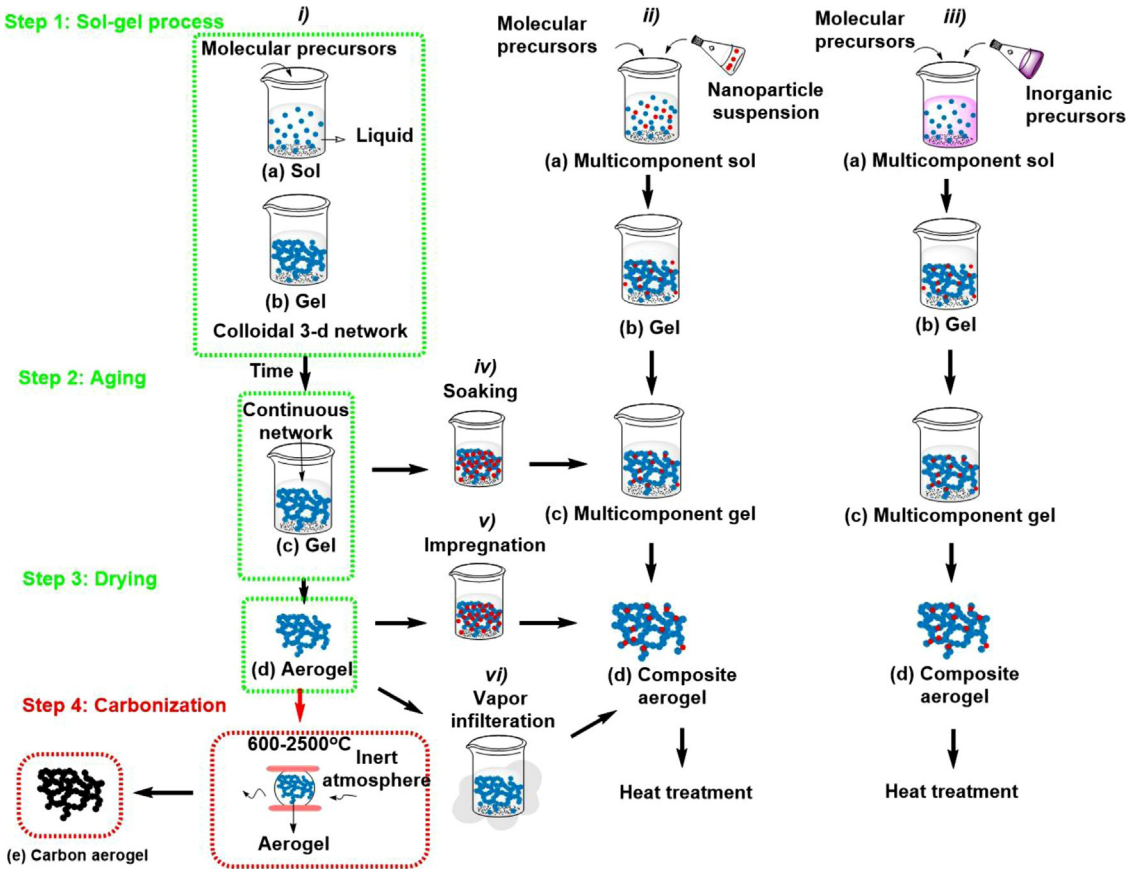

Fig. 2. Different procedures to prepare aerogel and aerogel composites based catalysts.

cation agents (*e.g.*, nitrates, phosphates), metal cations, *etc.* Major sources of water pollutants are those that originated from the textile and dye manufacturing, chemical and pharmaceutical industries, food technologies, oil refineries, petrochemical plants, and others [40]. Most of these contaminants are complex organic molecules or dyes that are often severely degraded or separated from the water sources. Several possible technologies based on physical, biological and chemical methods have been exploited to eliminate these organic water contaminants [2]. The utility of aerogels namely hydrophobic silica, carbon, cellulose, and biomass derived aerogels for water treatment has been promising not only from the aspect of physical and chemical adsorption but also with regard to the chemical degradation of the hazardous compounds through a series of the catalytic advanced oxidation process namely Fenton, Fenton like reactions as well as ozonation processes. In these processes, highly reactive species like hydroxyl radicals are obtained which are responsible for the degradation of aqueous pollutants.

For an efficient catalytic degradation of aqueous pollutants on aerogel networks, initial adsorption of contaminants from wastewaters would be extremely helpful. A high pollutant adsorption efficiency can often be achieved by tailoring the physicochemical and textural properties of the aerogel network, such as porosity, specific surface area, and surface hydrophobicity. In this respect, a recent review article by us has extensively studied the contaminants adsorption aspect of aerogels [2]. On the other hand, the mechanical strength caused by the interwoven network in aerogel prevents the loss of active catalyst or active surface area. Besides, crack free aerogel monoliths can host photoactive phases that could provide an efficient medium for photocatalytic oxidation of organic water pollutants.

This review gives an overview of all processes involved in the synthesis of different aerogel catalysts and catalyst supports and, in a broader sense, a summary of their recent applications as an environmental (photo)catalyst for removal of various pollutants from both air and water sources.

2. Synthesis

Basically, there are three steps involved in the preparation of aerogels including sol–gel reactions, aging and drying processes. In the case of carbon aerogels, an additional carbonization process is required [9].

2.1. Principles of sol–gel processing

The chemistry behind the formation of filigree aerogel network is based on sol–gel reactions. Generally speaking, a sol–gel reaction is a solution based synthesis that is accompanied by a transformation of a molecular precursor to a colloidal solution (sol) to obtain a solid material (gel) by the addition of a chemical crosslinker or by changing the physical conditions of the reaction *e.g.* pH, temperature. Fig. 1 schematically shows sol–gel reactions for the synthesis of materials in the form of nanoparticulate powders as well as self-supporting nanostructured monoliths having inorganic, organic and biobased molecular structures.

The sol–gel process can be adapted to both, aqueous and non-aqueous media [41]. Aqueous based sol–gel transition is basically the most predominant process and can be explained by the hydrolysis (formation of hydroxyl groups) and condensation reactions (formation of *e.g.* oxo bridges) of molecular precursors, *e.g.* metal alkoxides or inorganic salts, but also organic and

hybrid inorganic–organic monomers (M: metal, OR: alkoxy group) [42]. Silica-based sol–gel derived materials are a key example in this regard. Fig. 1 illustrates the sol–gel reaction of tetramethyl orthosilicate (TMOS) as a representative organosilane and its polymerization or polycondensation contributing in the formation of the 3D network build-up.

This figure also illustrates some typical non-hydrolytic condensation reactions in which instead of water, an organic oxygen donor *e.g.* alcohol, ether, carboxylic acid, *etc.* is used to build up oxo bridges in the network. This process is a simple and quite well-adapted procedure for the water-free synthesis of oxides and mixed oxides materials and involves a nucleophilic attack at carbon centers, *e.g.* condensation reactions accompanied by alkyl halide, ester or ether elimination [43]. This approach can also be extended to the synthesis of metal sulfides (chalcogenides) by using thiol and thioether sulfur-donors. However, a further explanation in this context is beyond the scope of this paper and the reader is conferred to the review of Mutin and Vioux [43] who have highlighted the pros and cons of non-hydrolytic reaction over conventional sol–gel reaction.

The sol–gel polycondensation to build up polymeric networks *e.g.* resorcinol-formaldehyde polymers proceeds analogously to purely inorganic polymers in the presence of a basic catalyst (*cf.* Fig. 1) [44]. Carbon or carbonaceous sol–gel based materials are also synthesized by carbonization or pyrolysis of the dried polymeric monoliths/materials. Fig. 1 also lists the typical representative monomers which are used to prepare carbonaceous monolithic materials [42,45]. For the biobased molecular precursors *i.e.* polysaccharides and polypeptides, the condensation proceeds in different ways through establishing physical interactions like hydrogen bonds between polymer chains by *e.g.* changing the pH of the media but also via chemical crosslinking by the addition of a crosslinker to the reaction [46]. The alginate-based polysaccharides condensation is an example of chemical crosslinking in which gelation can take place by the formation of linkages of the polymer chains with divalent cations (*i.e.* Ca^{2+}), following the so-called "egg-box" gelation model mechanism in which each cation is coordinated by the carboxyl and hydroxyl groups of four guluronate building blocks from two neighboring chains of the polymer (*cf.* Fig. 1) [46,47]. The 3D network obtained in here is called "aquagel" or "hydrogel" that could undergo a transformation into highly porous gels or powders.

2.2. Synthesis of aerogels – with an emphasis on aerogel catalysts

Unlike conventional approaches for preparing multicomponent heterogeneous catalysts that require precipitation and impregnation approaches, the sol–gel process offers a couple of attractive features that are not achievable with classical wet chemistry methods. A detailed overview of conventional synthesis approaches *i.e.* co-precipitation, impregnation, and hydrothermal synthesis, *etc.* is provided in an all-embracing review by Schwarz *et al.*[48]. Indeed, sol–gel processing is a straightforward approach which allows introducing several molecular precursors or even micro- or nanoparticles to the reaction mixture in a single synthesis step. As a product of the sol–gel reaction, we will focus on an overview of aerogel monoliths preparation. Apart from the chemistry, we will also give an outline of different synthesis approaches towards existing aerogels with an emphasis on aerogel-based catalysts and catalyst supports providing a detailed discussion of each synthesis step.

Until very recently, the most investigated materials forming fine aerogel structures are silica (SiO_2), polymers, carbon aerogels and various other types of aerogels together with their mixtures. If the functionality of aerogels was lacking the property demanded, additional components like molecules, metals, oxides or polymers were impregnated upon preserving the porous matrix.

Among the list of reported aerogels, single oxide aerogels (*e.g.*, Al, Ru, Ti, V, Cr, Fe, Sn, and Zr oxide) [49–51], binary/mixed oxides aerogels such as TiO_2–SiO_2 [52], ZrO_2–SiO_2 [53], Fe_3O_4–SiO_2 [54] and ternary composite aerogels such as V_2O_5–TiO_2–SiO_2, V_2O_5–Nb_2O_5–TiO_2 [55] as well as transition metal oxide doped aerogels containing Co, Cr, Mn, V, Fe, Cu, and Ni [56] have been prepared for various heterogeneous catalytic reactions.

Different synthesis approaches leading to the preparation of aerogels, and their composites have been sufficiently studied in several review articles by Hüsing et al., Baiker et al., Maleki et al. and in Handbook of Aerogels [1,9,16,57]. Fig. 2 summarizes schematically possible routes that have been proposed to prepare mixed oxides, metal, metal alloy doped metal oxides, oxide supported noble metals, as well as carbon and carbon supported noble metal aerogels which have been considered as heterogeneous catalysts and catalyst supports, so far.

According to the Fig. 2i, during the sol–gel reactions the first building blocks of the network with sizes of *ca.* 1–10 nm are formed, which can now grow or aggregate in the further process. This solution is referred to as "sol".

The primary particles are involved in polycondensation and further network growth to give larger secondary nanoparticles or bigger aggregates. These particles assemble to a three-dimensional nanostructured gel network which is accompanied by the sol-to-gel transition. The structural evolution and nanostructural build-up of the gel depends on the rate of hydrolysis and condensation reactions as well as other reactions parameters such as pH value, solvent type, water to alkoxide ratio, temperature and pressure [1].

Gelation does not imply that all precursors are consumed. Therefore, the wet gel as obtained from the sol–gel reactions is subjected to further aging processes. During aging, the network is left to grow further in the mother liquor with controlling parameters like pH value, temperature, and time. The aging parameters have a significant impact on the physical properties mainly in strengthening the delicate structure of the obtained gel through Ostwald ripening, coarsening, sintering and syneresis [58].

As all the aerogels are processed *via* wet chemical synthesis routes, the wet gels must undergo an appropriate drying process to obtain a highly porous, solid aerogel product. The liquid inside the gel structure must be removed without compromising the initial structure and dimensions. Several sub- or supercritical, freeze and vacuum drying approaches have been employed to remove the liquid inside the wet gels. The most common and to some extent, the benignest approach to dry the gel is the drying at ambient pressures after surface modification – which is well established for silica and carbon, and, to a lesser extent supercritical extraction with CO_2 ($scCO_2$) can be considered as a gentle approach due to its easily accessible critical conditions [58]. Usually, the wet gel structure collapses upon drying due to the high capillary stresses that act on the pore walls upon evaporation of the solvent. In this respect, the capillary stress can often be mitigated by anchoring an appropriate non-polar moiety to the pore surface *e.g.* methyl moieties and exchanging the pore liquid to *e.g.* hexane as a low surface tension solvent thus allowing to prepare crack-free monoliths [59]. In $scCO_2$ drying which is also called "cold process", the pore liquid is exchanged to supercritical CO_2 and therefore, there are no longer capillary stresses in the pores due to the disappearance of the menisci of the solvent in the pore walls at this point [60].

The carbon (C-) aerogels, which are prepared from carbonizable polymeric aerogels, *e.g.* prepared from resorcinol-formaldehyde (RF), undergo an extra processing step of "carbonization" immediately after drying. In this process, the organic aerogel is exposed to high temperatures (*e.g.* above 600 °C) in an inert atmosphere to decompose oxygen and hydrogen moieties of the polymeric chain, thus forming carbon networks according to synthesis route *i* in Fig. 2 [61].

In the synthesis routes *ii and, iii*, during the sol–gel process, several molecular precursors or even micro- or nanoparticles are introduced into the reaction mixture in a single synthesis step to be engaged in the sol–gel reaction. In these synthesis routes, the second phase will be distributed on or within the main network at both molecular and nanoscale level adding an extra property to the network without noticeably affecting the aerogel physical properties. Taking advantage of both synthesis routes, magnetite doped silica aerogels have been prepared by Maleki et al. [62], and Koebel et al. [63] to combine the properties of their constituents through the addition of magnetite nanoparticles into the prepared sol or mixing the iron salts with organosilanes along the preparation of the sol.

Additionally, deposition/precipitation of metal hydroxides on preformed wet gels by adjusting the pH of the solution, impregnation of preformed aerogel networks by a solution of a metal salt and, vapor phase deposition of metal particles on aerogel networks – synthesis routes *iv, v* and *vi* respectively – were regarded as straightforward approaches to prepare multi-component catalyst supports [57].

More recently, a major breakthrough was also made in the development of oxide free and metal-doped oxide free functional aerogels such as metal sulfides, selenides, tellurides (chalcogenide) by Brock et al. [64,65] which open enormous opportunities in various applications namely catalysis and photocatalysis. The development of pure metallic aerogels including Fe, Co, Ni, Sn, and Cu by a carbothermal method by Leventis et al. [66–68], but also the aerogels derived from quantum dots *e.g.* Au, Ag, Pt, and Pd as well as multimetallic including Au–Ag, Au–Pd, Pt–Ag, Pd–Ag, Pt–Pd, Au–Ag–Pt, Au–Pt–Pd, Ag–Pt–Pd, and Au–Ag–Pt–Pd by destabilization of their aqueous colloidal building blocks were reported by Eychmüller et al. [69–72]. Most of these exotic aerogels have also been considered for catalytic, electrocatalytic and bioelectrocatalytic purposes.

3. Aerogels in air cleaning applications

In the light of growing concerns regarding the ever-rising air pollution and subsequent global warming, different catalysts were explored to convert the various hazardous atmospheric organic and inorganic pollutants into less harmful compounds. In this respect, the contribution of aerogel catalysts from different molecular resources has been notable to protect and improve the environment from various hazardous pollutants. In this section, we highlight the application of aerogels for the catalytic and photocatalytic removal of air pollutants.

3.1. deNOx applications

Due to the harsh working conditions of the NOx abatement process, also called deNOx, the catalyst supports that are doped with the active species must display a good activity, selectivity, and a high thermostability. In addition, the catalyst support must have a large specific surface area even at high reaction temperatures *i.e.* at 800–1200 K [73].

The selective catalytic reaction of NOx by NH_3 is called SCR-NH_3, and the overall reaction in the presence of oxygen is presented according to the schematic reaction below [73]:

$$4NO + 4NH_3 + O_2 \rightarrow 4N_2 + 6H_2O \quad (1)$$

$$6NO_2 + 8NH_3 \rightarrow 7N_2 + 12H_2O \quad (2)$$

Among various metal oxide catalyst supports such as silica, zirconia, alumina, and titania, V_2O_5–TiO_2 is recognized as the most efficient one for SCR-NH_3 of NOx, today [74] especially when this catalyst is doped in trace amount with other oxides like WO_3 or MoO_3 to increase activity and stability [30,75].

In fact, V_2O_5–TiO_2 obtained by conventional synthesis approaches exhibits a good activity and selectivity toward formation of N_2 as well as an excellent resistance against poisoning by SOx that is usually discharged from the exhaust gases of the stationary combustion sources [6,76]. Various preparation methods for vanadia-titania catalyst, such as impregnation [77], precipitation [78], solid–solid wetting of TiO_2 with V_2O_5 [79], grafting from non-aqueous solutions [77,80] or chemical vapor deposition [77,81] have been studied. However, the TiO_2 support is only obtained with relatively lower mechanical and thermal resistance than other oxides *e.g.* silica, with rather low surface area. To overcome this problem, TiO_2 is processed via a sol–gel technique followed by a supercritical extraction for drying the material. This process can lead to the formation of TiO_2 aerogels with superior textural properties (*e.g.* high specific surface area and porosity) as well as an excellent catalytic activity [82]. In other words, the advantage of the aerogel catalyst arises from its high surface area which originated from the better preservation of the porous networks thanks to the supercritical drying. As the catalytic reactions take place on the surface, a high surface area in aerogel can, in principle, provide more active sites for heterogeneous catalytic reactions. Besides, a large surface area can better stabilize a catalytically active phase of a metal, or an oxide deposited on the surface [83].

Almost all vanadia-titania, V_2O_5–TiO_2, (V–T) mixed oxide aerogel catalysts have been synthesized through either the co-condensation method starting from molecular precursors and critical point drying (synthesis route *iii* – Fig. 1) or *via* two-step reaction of soaking a preformed titania gel with a vanadium solution – the alkoxide precursors diluted in isopropanol (i-PrOH) – and then the resultant gels were subjected to supercritical drying and calcination at temperatures of *ca.* 550 °C [27]. In addition, Engweiler and Baiker [82] reported V–T aerogel catalysts through chemical vapor deposition (CVD) of vanadia on the surface of preformed titania aerogels, similar to the synthesis route *vi* – Fig. 2, or through impregnation of titania aerogels with a non-aqueous solution using vanadyl tri-isopropoxide as a vanadium precursor, similar to the synthesis route *v* – Fig. 2. Generally, all mentioned strategies resulted in aerogel networks having core–shell type building blocks in which vanadia forms an outer shell to be easily involved in the catalytic reactions. It is thought that the vanadyl surface species (V=O groups) are responsible for the SCR.

Another reason for the enhancement of the catalytic activity on V–T aerogel is the good dispersion of vanadium oxide on TiO_2 which gives rise to the formation of "isolated" vanadyl centers [84] and "polymeric" polyvanadate species [85] on the surface, (*cf.* Fig. 3a*i–iii*). The semiconducting nature of TiO_2 is another asset for its high catalytic activity in SCR in which the d-orbital levels of vanadyl centers are located within its energy gap near to the conduction band.

Since 1970, several mechanisms for SCR have been investigated on vanadia-based catalysts [30]. Busca et al. [30] gave an overview of mechanistic pathways and the chemistry beyond the SCR-NH_3 of NOx over different oxide catalysts. Surface species are known to be involved in the reaction scheme of SCR and are identified by FTIR spectroscopy comprising molecularly adsorbed ammonia typically as ammonium ions over Brønsted acidic —OH surface hydroxyl groups (Fig. 3b *i*), or through Lewis-type interactions on unsaturated cations (*cf.* Fig. 3b *ii*) [86]. Fig. 3c indicates one possible mechanism of SCR on the V–T catalyst supports proposed by Janssen et al. [87] in which the intermediate species of V-ONH_2 is the key element in the SCR reaction.

The catalytic performance of V–T aerogels depends on the amount of vanadia loading and consequently increases with high

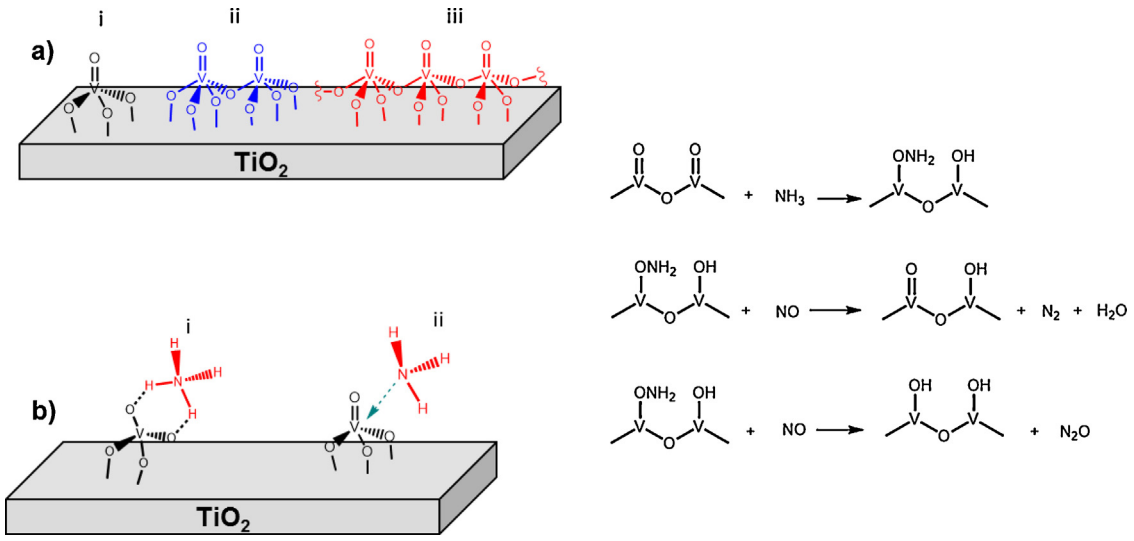

Fig. 3. (a) (i) Proposed structures for monomeric vanadyl species, (ii) dimeric and, (iii) polymeric metavanadate species in their dehydrated forms on the surface of V_2O_5–TiO_2 catalysts [85,88]; (b) (i) ammonium ions bonded at V Brønsted acid sites; (ii) Lewis-bonded NH_3 at vanadyl sites; (c) mechanism of the NO–NH_3 reaction on supported vanadium oxide catalysts proposed by Janssen et al. [87] in the presence of oxygen.

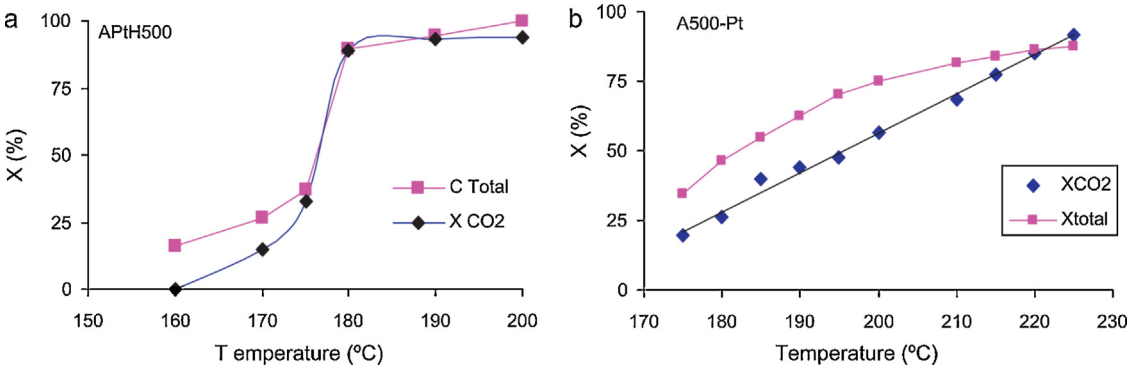

Fig. 4. Light-off curves for the combustion of (a) p-xylene and (b) acetone. 0.1 g catalyst, $F = 60\ cm^3\ min^{-1}$, [VOC] = 1500 ppm [122]. APtH500 are the Pt-doped carbon aerogels which were prepared by addition of $[Pt(NH_3)_4]Cl_2$ as Pt precursors to the initial polymeric solution and carbonized in 500 °C while, A500-Pt refers to the aerogel catalysts series which were prepared by impregnation (1 wt%) of the carbon aerogels by $[Pt(NH_3)_4]Cl_2$ as a precursor and followed by carbonization in 500 °C. Reprinted with permission from Ref. [122].

loadings [74]. It has been reported that the co-gelled aerogel converted ~83% of NO while this value for aerogels obtained from a two-step soaking route was 66.5% [74].

Baiker et al. [27] indicated that for the low-temperature (LT) SCR-NH_3 of NO, vanadia grafted on titania aerogels exhibited higher specific reaction rates (turnover frequency (TOF)) than vanadia grafted on SiO_2 or vanadia grafted on binary TiO_2–SiO_2 aerogel catalyst supports. The high catalytic activity of the titania catalysts was attributed to the high surface area and homogeneous loading with vanadia species. The low-temperature activity of V–T aerogels was significant with high loadings of vanadia, *i.e.* ~6–7 μmol V m^{-2}, and the catalytic activity remained constant up to 620 K. In contrast, V_2O_5–SiO_2, V_2O_5–TiO_2–SiO_2 even at higher loading of V_2O_5 deactivated during SCR up to 620 K, due to the lower acidity of the support. Kang et al. [89] showed that V–T aerogels could reduce up to 90% of NOx gas in the presence of oxygen over a wide temperature window. Besides the high active surface area, the high catalytic activity in these aerogels was attributed to the strong acidic sites as well as different vanadyl and polymeric vanadate species on the surface.

The SCR catalytic activity of V–T aerogel has also been reported to increase by doping 0.1% of ceria additives and exceeded to the maximum possible activity of ~95% by doping 1% W additive in the V–T–W ternary catalyst counterparts [76].

Carbon based catalysts have also been utilized for NOx abatement in last years as they are able to bring down the reaction temperature more than TiO_2 catalytic systems with presenting higher deNOx conversions [90]. However, carbon catalysts in the form of monoliths or membranes are of higher interest for this purpose due to their excellent and tunable physical properties [91].

The catalytic activity of carbon-based materials is correlated with both chemistry and textural properties, and both can be deliberately controlled by the synthesis and processing conditions *e.g.*, pH of the reaction, drying procedures and carbonization temperature [92–95]. Chemical functionalities on the carbon surface, namely oxygen groups with an acid or basic behavior and presence of heteroatoms (usually nitrogen functionalities) can be beneficial for support-active phase interactions, thus resulting in enhanced catalytic activity of the carbon materials toward NOx abatement [96,97]. On the other hand, the textural properties also contribute to the catalytic activity, and in this case, the most important textural properties are the surface area, as the surface area determines the number of available active sites for catalytic reactions, interconnected mesoporous structure and modifiable pore size distribution [98]. The carbon-based catalyst when impregnated with different

active phases of Cu [99], Fe [99,100], Mn [101,102], and V compounds [96,103] can contribute in SCR deNOx process having low optimal reaction temperature. The activated carbon-based catalyst containing vanadium as an active phase (using coke ashes as V source) has been extensively studied by Lazaro et al. [96,104,105]. They found that the textural properties like surface area, porosity, and the presence of surface oxygen groups can be decisive on the stable fixation of vanadium on the carbon surface. The SCR-deNOx process in the presence of ammonia and O_2 and vanadium supported carbon catalyst (3wt% V-load) was increased with the highest number of surface groups. In some cases surface treatment of carbon catalyst with HNO_3 yielded higher NO conversion, achieving almost 90% conversion [96]. It has been reported that ammonium chemisorption on the V center of the catalyst as well as on the oxygen functionalities (carboxylic acids moieties) was a key step in the overall deNOx mechanism of reaction [106].

Despite the high utilization of activated carbon, carbon nanofiber and ordered mesoporous carbon materials (OMC) [90], carbon-based aerogels or xerogels specifically has very limited studies for the SCR-deNOx process in the literature. However, carbon xerogels have been contributed in NO abatement through an oxidation of NO to the higher oxidation state of NO_2 at room temperate; subsequently, the produced NO_2 was captured in water as nitric acid moieties [98]. In this context, different carbon-based xerogels have been investigated which was prepared by the reaction of resorcinol and formaldehyde by varying the pH of the reaction, and subsequent drying and calcination under various temperatures. The calcinated carbon xerogels were chemically treated on the surface with urea or oxidized with nitric acids to enhance surface active sites like nitrogen and oxygen groups with a moderate alteration in the textural properties. Although the oxidative treatment has less effect on the catalytic activity, the urea treatment enhanced the catalyst performance and increased the NO oxidation at relatively low temperatures. Also, the highest catalytic oxidation of NO have been achieved with samples contain the highest surface area ($\sim$714 $m^2\,g^{-1}$) [98].

3.2. VOCs combustion

Volatile organic compound corresponds to the organic entities with the low boiling point that causes a large amount of solvent to evaporate from a liquid state or to sublimate from the solid state of compounds and enter to the surrounding airs with relatively high vapor pressure [107]. VOC is very toxic for both human and the environment. Therefore, their removal is an urgent need. Catalytic combustion of VOC is recognized as the most efficient and environmentally benign approach due to its low operation temperature (around 250–500 °C) with less NOx formation when compared to the conventional thermal oxidation methods [108]. VOC combustion catalysts contain noble metals (Pt, Pd, Rh, Au, Ag), transition metal oxides (Ni, Cu, Co, Cr, Ti, Fe, *etc.*), as well as their combinations (*e.g.* MnO_x–CuO_x, MnO_x–CeO_2) as nano or microscale particles homogeneously dispersed on highly porous oxides such as carbon, alumina or silica [34,109–119]. The catalytic performance of a catalyst in VOC combustion has been determined by (i) intrinsic properties of active phase (*e.g.* dispersion, loading, oxidation state, *etc.*), (ii) characteristics of support (*e.g.* porosity, hydrophobicity), and (3) operating parameters (*e.g.* concentrations of VOC, VOC type, flow rate, reactor type) [120].

Catalyst based on the noble metals is more preferential and practical for combustion catalysis of VOCs due to the high catalytic activity, resistivity to deactivation and possibility of regeneration [113,121]. However, high costs, as well as sensitivity to the poisoning by chlorine or chloride compounds, have limited their industrial applications. Instead, transition metal oxide based catalysts display less activity while are more efficient regarding cost.

Aerogels, in general, are recognized as the suitable candidates for the adsorption/absorption of VOC vapors from effluents due to their tunable textural *e.g.* high specific surface area and porosity and structural properties *e.g.* density and monolithic structures as well as tunable surface chemistry [122,123].

Some aerogels like carbon, transition metal oxide, and mixed oxides aerogels combined with noble metal catalysts, such as Pt, Pd, *etc.*, have been proposed as combustion catalysts for removal of VOCs [26]. However, carbon aerogels have presented better catalytic performances for VOCs combustion compared to the metal oxides due to the number of reasons: (1) the hydrophobic character which allows performing VOC combustion at relatively low temperatures with minimum water vapor chemisorption on the catalyst surface, (2) the tunable textural properties that allow for the homogeneous and high dispersion of the active metal phase on the support along with a good adsorption performance of the support toward VOCs [122,123]. However, the size of porosity in carbon aerogels must be adjusted through controlling the sol–gel parameters, carbonization and activation conditions in such a way that metal particles retain their catalytic activity [124].

Various methods such as impregnation, doping, equilibrium adsorption, CVD, *etc.* are investigated to deposit the noble metal on carbon aerogels. Among these methods, the doping the initial organic solutions is recognized to be highly efficient, as the probability of sintering and the loss of active phase by leaching is very low [125]. The important feature of metal-doped carbon aerogel is relying on its ease of preparation which is normally carried out by the addition of a soluble metal salt to the initial organic mixture. After gelation, the metal ions are entrapped inside the gel structure and chelated by the organic functional groups of the polymer matrix. The entrapped metal ions inside the gel structure vary the degree of polymerization in the polymer matrix, and as a consequence, an alteration in some textural properties in filigree aerogel *i.e.* pore size and morphology occurs. After carbonization, the metal phase is distributed homogeneously through the porosity of the carbon aerogel [124]. Therefore, it is expected that organic aerogels greatly determine the homogeneity of metal phase distribution on carbon aerogels and textural properties as a first obtained solid material.

Maldonado-Hódar et al. [126] prepared platinum-containing carbon aerogels through two strategies: (1) impregnation of preformed carbon aerogels with the Pt coordination compound $[Pt(NH_3)_4]Cl_2$ (A-series catalyst) or (2) through mixing the $[Pt(NH_3)_4]Cl_2$ precursors with the initial organic monomer mixture and followed by pyrolysis to obtain carbon aerogels (B-series catalyst). In the case of the A-series, the catalyst was pretreated with H_2/He in order to develop a metallic Pt in a carbon matrix, while in the case of B-series, the metallic Pt were obtained during the heat treatment of carbonization process. The toluene combustion performance of the prepared catalysts was studied by conversion *versus* reaction temperature (light-off curve) and conversion *versus* reaction time at different toluene concentrations. The light-off curve in case of the A-series catalyst indicated that the total toluene conversion shifted to lower temperatures by increasing Pt particle sizes while in the case of B-series catalyst the reverse happened. These two different combustion behaviors were ascribed to the difference in the dispersion pattern of Pt in both catalyst series and the availability of surface active centers at certain particle sizes and encapsulation of active sites in the carbon matrix.

The adsorption behavior in metal-doped carbon aerogel is varied and influenced by textural properties such as micropores volume, their size distribution as well as surface chemistry and hydrophobicity which are all controlled by the carbonization temperature [122]. In the study by Maldonado-Hódar et al. [122], two series of Pt/carbon aerogels (1% Pt loaded in catalyst) through impregnation and doping approaches were prepared. The performance of these series of aerogels on both catalytic combustion and adsorption

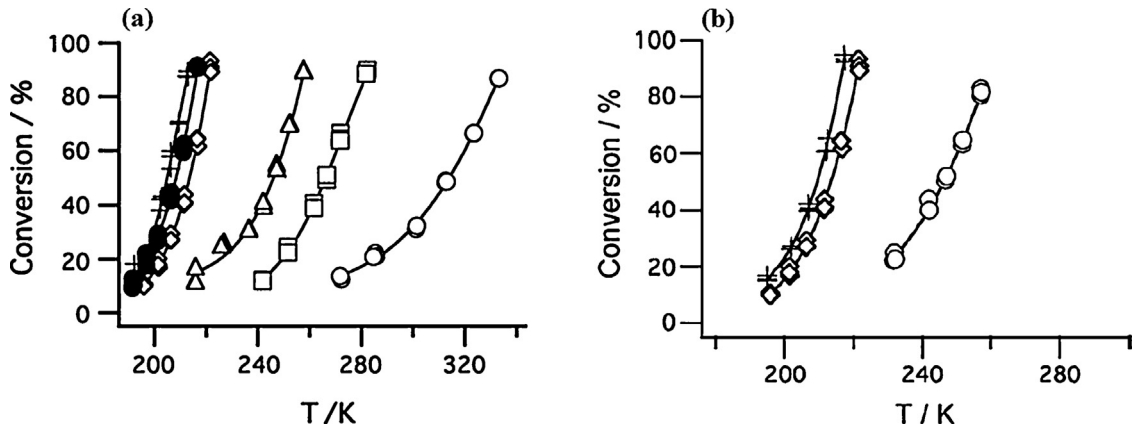

Fig. 5. Temperature dependence of (a) the CO conversion for the samples having Au loadings of 0.14 (○), 0.39 (□), 0.93 (△), 5.2 (◊), 9.6 (●), and 20 (+) wt%, (b) temperature dependence of the CO conversion for 5.2 wt% samples calcined at 673 K (◊) for 4 h and then further calcined at 973 K for 2 (+) and 4 (○) h. Reprinted with permission from Ref. [154].

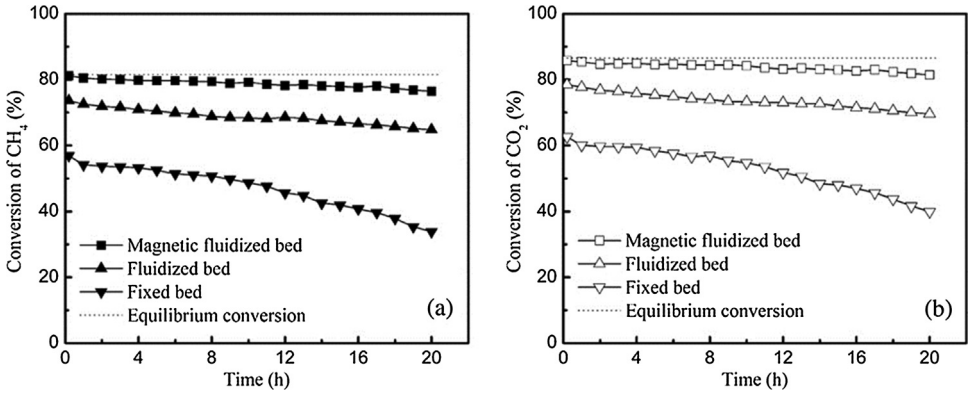

Fig. 6. (a) Conversions of CH_4 and (b) CO_2 as a function of time on stream over the 20 wt.% Co/Al_2O_3 aerogel catalyst under the three types of reactors. Reaction conditions: 973 K, 0.1 Mpa, 0.12 g catalyst, 150,000 ml/h g, $n(CH_4):n(CO_2):n(N_2) = 1:1:1$, H = 320 Oe. Reprinted with permission from Ref. [178].

abatement of aromatic and oxygenated VOCs were almost different and influenced by their preparation method and textural and chemical properties. Increasing the carbonization temperature from 500 to 1000 °C positively influences the adsorption capacity of toluene which showed the lowest polarity among the studied VOC. This was true for the static adsorption behavior of the catalysts at room temperature while in the case of dynamic adsorption condition the adsorption capacity decreased continuously with increasing reaction temperature up to the 200 °C due to the effect of temperature on the pore size distribution of aerogels [122]. The higher the carbonization temperature (>1000 °C) the more thermally stable become the aerogels because the weaker bonds were gasified and only the thermally robust C—C bonds remain in the solid matrix. Fig. 4 indicates the light-off curves of aerogel catalysts for the combustion of p-xylene (a) and acetone (b). The figures are based on the VOC disappearance (X_{total}) and the CO_2 conversion due to the selectivity of combustion to the CO_2 formation and it is reported that $CO_2 + H_2O$ are the productions of C/Pt combustion of VOC [127]. In most cases, irrespective of the type of VOC, at low temperature the X_{total} is greater than which is due to the high adsorption of VOC on carbon aerogels. As shown in Fig. 4, the total combustion of aromatic p-xylene took place at relatively low temperatures (~180 °C) while in the case of acetone only 25% of VOC were destructed or converted to CO_2 at this temperature. This is because of the reactivity pattern in two phases, as well as weakness in C—H bonds which vary in different VOC on the Pt/C catalysts.

It is noteworthy to mention that the main factor to determine the reactivity of volatile organic compounds in oxidation catalytic reactions is the strength of C—H bonds in the compounds. On the supported platinum catalysts, the compounds with single C—H bonds are basically more prone to the destruction by catalytic combustions. The reactivity of various volatile organic compounds having different functional groups has been studied over platinum catalysts supported on a range of (non-aerogel) inorganic supports like β-zeolite, mordenite, silica or alumina. The oxidative destruction of a range of organic molecules namely alcohols, ketones, carboxylic acids, aromatics, and alkanes was assessed. The observed reactivity pattern was alcohols > aromatics > ketones > carboxylic acids > alkanes. And, as long as the volatile organic compounds are involved, the adsorption also might become the main factor leading the oxidative destruction occurs at lower temperatures [128].

Noble metals supported on different non-aerogels transition metals such as γ-Al_2O_3, SiO_2, TiO_2, ZrO_2, Fe_2O_3, CeO_2, MnO_x, *etc.* unlike to their aerogel counterparts, have been extensively reported [129–133]. In most of these non-aerogel catalysts, catalytic performance has been influenced by precursor types and eventual support characteristics such as acidic or basic behavior, hydrophobicity, and porosity [123]. For instance, the acidic strength in supports such as γ-Al_2O_3, SiO_2, ZrO_2, improved the catalytic performance of their noble metal supported catalysts [134,135]. Also, among the noble metals, Au nanoparticle has been reported for its exceptional catalytic performance for VOC combustion as it can be highly dispersed on the metal oxides supports such as Fe_2O_3, Co_3O_4, CeO_2, TiO_2, and Mn_2O_3 [129,136,137]. However, in this case, the catalytic activity of Au supported catalysts was drastically influenced by the size of Au nanoparticles and type of support

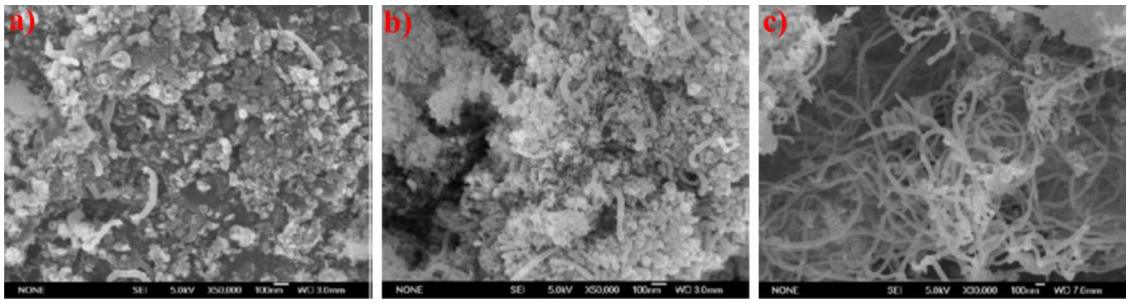

Fig. 7. FE-SEM images of the catalysts after 20 h operation, (a) in the magnetically fluidized bed, (b) in the fluidized bed and (c) in the fixed bed. Reprinted with permission from Ref. [178].

Table 1
Physicochemical properties with the catalytic performance of Ni(20 wt%)/Al_2O_3 catalysts.

Ni(20 wt %)/Al_2O_3 catalyst	Density ($cm^3\ g^{-1}$)	Specific surface area ($m^2\ g^{-1}$)	Ni crystalline size (nm)	Catalytic performance (CH_4)%	Carbon deposition amount (wt% of catalyst)
Aerogel	0.05	195	9.2	~95% (30 h)	14.6
Xerogel	130	130	13.5	~45% (30 h)	26.7

which both were controlled by the synthesis method and processing conditions [138]. Among the oxides mentioned above, there are also few studies concerning utilization of their aerogels such as vanadia–titania [139], chromia supported noble metals and transition metal oxides [26], and alumina foam coated chromia [140] for catalytic oxidative removal of halogenated and non-halogenated VOCs.

Choi et al. [139] applied vanadia–titania aerogels for the oxidative decomposition of 1,2-dichlorobenzene (DCB) as an example for a chlorinated aliphatic hydrocarbon which is of major risk for the environment and human health. The catalytic oxidation of DCB was conducted in the temperature range of 150–600 °C with attaining 90% conversion at 450 °C without deactivation of the catalyst during 48 h of operation. Also, the catalytic activity of vanadia–titania aerogel remained almost constant after conducting four different oxidation cycles, and carbon oxides were the sole product in all temperature ranges. The catalytic activity in vanadia–titania aerogels was attributed to the high specific surface area and homogeneity in the distribution of mono and polyvanadate species on the catalyst surface especially when the anatase phase of titania supports was used.

3.3. Preferential oxidation (PROX) of CO

An ideal catalyst for CO-PROX must be highly active, stable and selective for CO-PROX in the H_2-rich gas stream and operates at lower temperature ranges [141]. Several promising catalysts for the CO-PROX process based on supported noble metal catalysts such as Pt, Pd, Ir, Ru or Rh [142–145], nano-gold catalysts [146–148], and metal oxides catalysts [149–151] have been reported.

Compared to conventional catalysts which were prepared by impregnation of catalyst to an oxide substrate, inorganic aerogels are excellent candidates for the CO-PROX as they exhibit some desirable characteristics such as inertness, high specific surface area, mesoporosity and good thermal stability [152]. In this context, alumina and silica aerogels loaded with the active metals such as platinum, cobalt, platinum–cobalt bimetallic species [152,153] and gold nanoparticles [154] were used for CO-PROX from an H_2-riched stream. Although silica aerogel supports have superior characteristics than alumina supports concerning their high specific surface area that allows for a good dispersion of noble metal active sites without minimum interaction as well as high reducibility of metal oxide on silica as compared to that of the alumina. In the CO-PROX process, the selectivity toward CO oxidation/removal as well as catalytic activity at lower temperatures is very important which can be controlled by the catalyst preparation methods as well as the starting materials/precursors. For example, Kwak et al. [153] investigated the catalytic performance of bimetallic Pt–Co on alumina aerogel, and xerogel catalyst supports that were prepared through a single stage sol–gel process. They have found that a synergetic effect of platinum and cobalt conferring an improved catalytic performance toward the oxidative removal of CO. Also, the catalytic activity of the aerogel was better than that of the xerogel catalyst due to the preservation of well distributed Pt–Co bimetallic active sites in the alumina structure upon supercritical drying. Indeed, ambient pressure oven drying led to large shrinkages and collapse in the gel structure causing a redistribution of the active metal sites on the support and therefore leading to a nonuniformity in the catalyst. It has also been shown that PtCo-aerogels reduced the outlet concentration of carbon monoxide to below 10 ppm in a wide temperature range of 75–200 °C [153]. The onset temperature was lower than that in the case of PtCo-xerogel without consumption of H_2.

Choi et al. [152] also developed Pt and Co–Pt-silica aerogels by adsorption of platinum and cobalt ions (H_2PtCl_6 and Co^{2+}) on preformed wet silica gel structure through a post-synthesis solvent exchange adsorption. Due to the strong interaction between $PtCl_6^{2-}$ anion and cobalt cations in the sol state the bimetallic Pt–Co species were obtained. The distribution of active species of Pt and Co in the aerogel structure has been influenced by the type of metal precursors and type of used solvents. In aerogels prepared by a post gelation soaking procedure, Pt and Co tended to agglomerate in a co-existing site as Co–Pt bimetallic species by controlling their surface charges as well as using DMF aprotic solvents. DMF as a solvent stabilized the platinum ion ($PtCl_6^{2-}$) sites and increased its affinity to link with positively charged Co species. The major role of Co in Co–Pt doped aerogels was to increase the reducibility of Pt and rendering it to become more stable in its reduced state and therefore enhance the catalytic activity by shifting the CO-PROX to the lower temperatures [152]. The resulting aerogels possess a catalytic activity for CO-PROX process from H_2-riched fuel in a wide temperature range of 25–300 °C.

Au nanoparticle supported metal oxides also possess an impressive catalytic performance for the CO oxidation at a lower temperature when their diameters are less than 5 nm [155]. Tai and Tajiri [154] reported the preparation of an Au/titania–silica

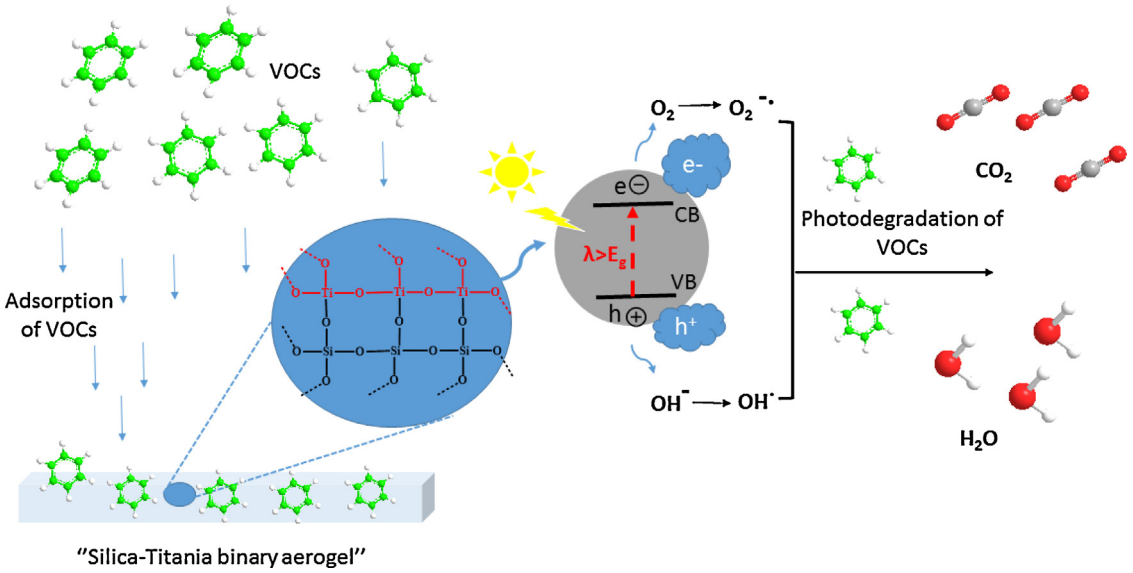

Fig. 8. Mechanism of heterogeneous photocatalysis reaction on the aerogel structure in the gas phase. *Note*: benzene is a model VOC compound, and silica–titania aerogels are model aerogel photocatalysts.

Table 2
Aerogel catalysts used in the methane reforming by CO_2 and their performances.

Aerogel catalyst	Operation mode	CH_4 conversion (%)	Deactivation mechanism	Remarks	Ref.
$NiO–La_2O_3–Al_2O_3$	Fixed-bed reactor	• 96% at 1173 K after 20 h reaction	Slight carbon deposition on the catalyst surface	• Homogeneous distribution of bonded Ni-ions on the support • Introducing the La_2O_3 increased the adsorptive capacity of CO_2 by aerogels and facilitated its interaction with NiO active sites	[180]
Ni/Al_2O_3	Fluidized-bed reactor	• Depending on the Ni loading (90% for a sample with 10% Ni loading after 48 h reaction)	Limited graphitic carbon deposited on the surface	• The aerogel catalysts exhibited high specific surface areas, low bulk density, small Ni particle sizes, strong metal–support interaction, high Ni dispersion and low rate of carbon deposition	[181]
Co-Ni bimetallic	Fixed-bed reactor	• Depending on the Co/Ni ratio • (5Co/5Ni) contained the highest conversion of 79% and remain stable after 30 h reaction	Coke deposition increased by decreasing the Co/Ni ratio	• Synergic effects of the lower coke formation rate, the smaller metal particle size and stronger metal-support interaction of the catalyst were achieved by higher Co/Ni ratios.	[171]
$Co-Al_2O_3$ granules	Fluidized-bed reactor	• CO_2 conversion reached equilibrium after 6 h and decreased 7% after 25 h operation time	Deactivation due to carbon deposition was not significant in case of granular aerogels	• The granulated aerogel catalyst showed better catalytic stability and greater conversion of methane as compared to the non-granulated • aerogel catalyst. Granulation improved solid-gas contact efficiency.	[182]

aerogel catalyst system and investigated its catalytic performances toward CO-PROX. Au nanoparticles at a size range of *ca.* 2 nm were distributed and entrapped on the porous amorphous structure of titania-coated silica aerogels. The Au nanoparticles (with a loading of up to 10%) were well dispersed in the catalyst and thus, no longer subjected to sintering or agglomeration. Fig. 5a shows the CO conversion reactions for different Au loaded titania–silica aerogel catalyst samples obtained from various calcination temperatures. The catalyst containing Au loadings higher than 0.5 wt% had a better catalytic activity at temperatures even below room temperature. The temperature at which the conversion was 50% ($T_{1/2}$) decreased with increasing Au loading. In fact, oxidation per catalyst increased monotonously with increasing Au loading for the Au/titania–silica aerogel catalyst samples. Also, when this catalyst was subjected to a calcination process for 2 h at 973 K, not only its catalytic activity did not decrease, but also it was slightly more active than when it was subjected to calcination at 673 K. This catalytic behavior will be guaranteed when the diameter of Au nanoparticles is taken into account. Moreover, Au nanoparticles were still capable of retaining their sizes to below 5 nm when the catalyst was subjected to the additional calcination up to 10 h at 973 K and catalyst still indicated total CO conversion below 273 K [154] (Fig. 5b).

3.4. Methane reforming with CO_2

The primary purpose of methane reforming with CO_2 is to produce synthesis gas (syngas) with high H_2/CO ratio according to the following reaction

$$CH_4 + CO_2 \rightarrow 2H_2 + 2CO \quad (3)$$

Apart from the hydrogen production as a clean energy source, the resulting syngas can be used for the production of liquid fuels such as methanol or diesel in Fischer–Tropsch plants [156]. However, methane (CH_4) reforming with CO_2 is also considered as an

efficient way to minimize the two most problematic greenhouse gases, such as CH_4 and CO_2, and convert them into the beneficial synthesis gas and clean energy [157,158]. Indeed methane reforming with CO_2 can minimize the impact of large-scale CO_2 emission from fossil fuel power plants and in ammonia synthesis industries and in turn abate the problems with regards to the limitation in the large-scale CO_2 storage and sequestration [28].

It is well known that noble metals such as Pt, Pd, Ru, as well as other transition metals like Ni and Co can be used to catalyze the above-mentioned methane reforming process [159]. The noble metals, in general, show the highest activity and stability with respect to the deactivation due to carbon deposition on their surface [160]. However, the high costs and limited availability of noble metals have restricted their application. From a practical point of view, other metals such as Ni and Co and their bimetallic system [161] have been more actively investigated for methane reforming because of their high activity and abundance although they are more prone to deactivation caused by the coking or carbon deposition on their surface, as a result of sintering the metal phase on the support to prepare a bigger ensemble of metal as a nucleation site for the carbon deposition [162]. Carbon deposition or coking on the catalyst surface during CO_2 reforming of CH_4 is recognized as an unavoidable phenomenon for the high C/H ratios in this process. Attempts in recent decades to mitigate this problematic issue are based on controlling the catalyst preparation and structural parameters such as the specific surface area, the size of active metal on the catalyst supports and type of catalyst support *e.g.* xerogel *vs.* aerogel [163–166].

Recent studies revealed that nanoparticle catalyst exhibits a better catalytic performance due to their unique morphological and physicochemical properties which lead to a high dispersion of the active metal phase on the support [162,167]. These catalysts can be prepared with a number of methods such as impregnation, co-precipitation or sol–gel processes [168–170]. Among these preparation methods, the sol–gel technique in tandem with supercritical drying has been known as very effective because the resultant metal oxide aerogel catalysts have shown an improved catalytic behavior which is due to the high dispersion of metal on the aerogel support as well as its strong interaction with support, leading to great activities as well as low coking rates in methane reforming reactions [166,171–173].

Osaki et al. [174] prepared monolithic nickel–alumina ($NiO–Al_2O_3$) aerogel catalysts for CO_2 reforming of methane. After calcination and H_2 reduction of the catalyst, the $Ni–Al_2O_3$ catalyst was obtained with a uniform distribution of Ni throughout Al_2O_3 by making Ni—O—Al bondings. A better catalytic performance and lower probability of catalyst deactivation by coking and metal sintering in the co-gelled mixed oxide aerogels was observed compared to a catalyst that was obtained by a conventional impregnation method at a same loading of NiO. In addition, an aerogel catalyst preparation by co-gelation of two different precursors allowed to tune the size of the metal oxide particles by changing the initial Ni ion concentration in the precursor solution in order to prevent the nucleation of the carbon in the active metal sites. In this respect, Kim et al. [166] optimized the metal particle size with which the high activity and low coking rate for the Ni-alumina catalyst were obtained. They found the sol–gel technique to be the most appropriate to optimize the metal loading content and its size on the catalyst. The evolution of the filamentous carbon species on the catalyst surface and its subsequent deactivation were attributed to the formation of the large particle sizes of Ni (>7 nm) on the conventional catalyst, or Ni impregnated catalyst during preparation and additional sintering in the post-synthesis steps [166]. Whereas aerogel catalyst due to the good textural properties and high thermal stability (up to 973 K) was resistant to the carbon deposition and deactivation.

On the other hand, another important parameter that strongly influenced the carbon deposition is the operation mode regarding implementing a particular type of reactor *e.g.* a fixed-bed *vs.* fluidized-bed reactor especially when the aerogel nanostructured catalyst is used [163–166].

Recent investigations have shown that conducting the reforming process in a fluidized-bed reactor can increase the contact of the catalyst particle with gas due to the constant circulation and motion of the catalyst particle and gasification of the deposited carbon. Therefore, a substantial resistance to the carbon deposition on the catalyst surface can be attained [175]. However, for aerogels, fluidizing the catalyst in the fluidized-bed reactor is not readily possible due to the strong cohesive forces between the particles, [176] and in this case implementing a magnetic/electric field or ultrasound assisted fluidized-bed reactor has proven to be useful [175,177]. Hao et al. [178] improved the fluidization quality of Co/Al_2O_3 aerogels by introducing an axial uniform magnetic field to the reactor. As can be seen from Fig. 6, the magnetic fluidized-bed reforming exhibited the best catalytic activity among the conventional fluidized and fixed-bed reactors during 20 h reforming reactions. Moreover, the catalyst in the magnetic fluidized-bed exhibited the highest initial conversions of CH_4 and CO_2, which were close to the thermodynamic equilibrium condition, although the CH_4 conversion decreased slightly from 81% to 76% by increasing the operation time to 20 h (*cf.* Fig. 6a). Additionally, SEM micrographs (*cf.* Fig. 7a–c) of catalysts after 20 h operation revealed that the morphology of deposited carbon on the magnetically fluidized bed was entirely different, appearing as small filamentous carbon species compared to the long filamentous graphitic carbon in the conventional fluidized and fixed bed reactors (Fig. 7).

Specific surface area and the density of catalyst are also necessary for the methane reforming process [175,179]. For example, in the case of $Ni–Al_2O_3$, a high fluidizing quality and a less coking problem for aerogel catalysts were observed when compared to their xerogel counterparts. As indicated in Table 1, both catalysts indicated different properties regarding Ni crystalline size, density, specific surface area, along with their catalytic performance and percentage of evolved filamentous carbon on the catalyst surface. In the case of aerogel, upon calcination at 650 °C, Ni species were homogeneously dispersed on the Al_2O_3 through forming a stable $NiAl_2O_4$ spinel structure while in the case of xerogel, a poorly distributed Ni having isolated NiO besides $NiAl_2O_4$ spinel supported on Al_2O_3. The catalytic performance with regard to the conversion of methane and CO_2 and selectivity toward CO and hydrogen was much better in the case of the aerogel (20 wt% Ni loading) which was attributed to the outstanding physicochemical properties like a low density and high specific surface area in aerogel.

Table 2 lists the different aerogel catalysts that have been used in the methane reforming process by CO_2 and their respective catalytic performance in more detail.

3.5. Photocatalysts in air cleaning

The concept of pollutant photocatalysis involves in the mineralization of organic compounds to convert them into CO_2 and H_2O by exposing the photocatalyst to UV (Vis) irradiation under ambient temperature and pressure [183].

In a heterogeneous photocatalytic process, large specific surface area to provide active sites for adsorption and interfacial photoreaction events, high porosities to facilitate the mass transport of liquid and gaseous species, and a 3D interconnected network to provide continuous charge transfer and increased light harvesting ability, are desirable [184].

Based on the fact explained above, apparently, aerogels are proper candidates for photocatalytic applications [185]. For instance, native TiO_2 is considered as an efficient and relatively

inexpensive and benign photocatalyst with notable photocatalytic efficiency toward degradation of various air and water contaminants. However, a wide band-gap energy which only allows absorption of UV light, and the low surface areas have limited its efficiency in photocatalytic reactions [186]. Processing of TiO_2 into aerogel monoliths with the sol–gel process followed by supercritical drying and heat treatment, not only provides a control of the microstructural properties to obtain high surface area and tunable nanoporosities but also generates a desired photoactive nanocrystalline phase of TiO_2 (anatase) [187–191]. Doping with other photoactive semiconductors can modify the band gap, inhibits a fast photogenerated electron–hole (e^-/h^+) recombination and improves the photoactivity of TiO_2 [186,192,193]. On the other hand, as in the heterogeneous catalysis, the reaction takes place on the active surface of the catalyst, the photoactivity of TiO_2 can be further enhanced if the photocatalyst adsorbs more of the targeted pollutants. The adsorption capacities can be strengthened when the heterogeneous photocatalysts are processed into 3D and free standing robust porous aerogel structures [193].

As depicted in Fig. 8, in a gas-phase photocatalysis process on an aerogel structure, several critical steps are involved. The first step is the adsorption of VOC compounds or other organic contaminant species to the porous aerogel surface which is followed by activation of its photoactive surface by UV radiation to generate electron–hole (e^-/h^+) pairs. Afterwards, the reaction between adsorbed species on the surface and free radicals (*i.e.*, $OH^\bullet$) which are produced by trapped electron–hole pairs takes place in order to degrade the adsorbed species. Finally, the degradation products are desorbed from the surface [123].

The processing of TiO_2 into a crack-free free standing aerogel monoliths is quite an intricate process as TiO_2 monoliths tend to rapidly collapse to powders after supercritical drying due to their meager mechanical strength [194]. For this reason, in several case studies, molecular-level mixed TiO_2–SiO_2 binary aerogels have been prepared by adjusting the rate of hydrolysis of the two alkoxide precursors during the sol–gel process [194] or by impregnation of silica alcogel with titania alkoxides [195] followed by supercritical drying and heat treatment processes. TiO_2–SiO_2 binary aerogels show mechanical strength but are also catalytically active as well as selective toward isomerization and epoxidation reactions [16] and have also indicated a substantial photocatalytic degradation activity in both gas and liquid phases [196]. However, crack formation, and non-uniform spatial distribution of titanium in these binary oxide monoliths are a challenge especially for titania–silica aerogels with Ti/Si ratio > 0.1 [197].

Despite its mesoscopic pore size, large surface area and monolithic structure, pure silica aerogels are photocatalytically inactive. The as-prepared binary silica–titania aerogels processed from CO_2 supercritical drying are also inactive for photocatalytic oxidation of air pollutants due to their amorphous structure. Only after calcination at high temperature ($723\ K < T < 1023\ K$) after CO_2 supercritical drying the active polymorph anatase is accessible. Another alternative would be to use high-temperature supercritical drying with solvents, such as ethanol or acetone, or the assembly of preformed crystalline nanoparticles into 3D aerogel networks.

Additionally, the size of titania nanocrystalline domains is equally important and must be in the range of average diameters of 10 nm, obtained from peak broadening of XRD, or 7 nm, obtained from TEM micrographs [198].

The TiO_2–SiO_2 aerogel (Ti/Si = 1) prepared *via* sol–gel processing and supercritical drying with ethanol led to the formation of crystalline anatase titania nanophases which were anchored to the network through the creation of Si—O—Ti bonds and provided an active medium for capture and photocatalytic oxidation of the VOC compounds such as isopropanol and trichloroethylene [194].

In another study, binary titania–silica aerogels with high content and homogenously distributed titanium centers and the relatively high active surface area ($650\ m^2\ g^{-1}$) have been prepared through supercritical impregnation of titanium alkoxides into a silica alcogel followed by supercritical drying and calcination processes [199]. The microscopic investigation confirmed the presence of anatase (TiO_2) aggregated on the catalyst surface when the supercritical solvent, calcination temperature, impregnation and preparation parameters were properly controlled. In the case of supercritical drying with ethanol as the solvent, the formation of photocatalytic active anatase TiO_2 phases resulted, whereas supercritical drying with CO_2 led to the formation of photocatalytic inactive amorphous structures. The binary titania–silica aerogels derived from supercritical drying with ethanol had a suitable adsorption capacity in the absence of light with a proper photocatalytic performance in the presence of light for decomposition of benzene as a selected VOC [200].

Additionally, pore sizes and their size distribution are other important criteria in photocatalysis, as uniform pore sizes may provide higher active surface area and more active sites, which could be attained through the sol–gel process coupled with templating approaches [193]. This has been addressed by Yao et al. [201] with studying the effect of different mesophases of surfactant-templated titania–silica aerogels on the photooxidation ability of VOCs and indoor air contaminants. Additionally, the variation of the titania contents in the aerogel photoreactor has been studied. According to this study, the binary aerogel (Ti/Si = 0.75) prepared *via* supercritical extraction with ethanol and with an ordered mesophase pattern and a well-defined hierarchical porous structure having a uniform distribution of titania in the aerogel network shows the best performance. The titania–silica aerogel (Ti/Si = 0.75) developed in this study, has demonstrated ordered microdomains of titania with a larger pore structure which resulted in 15 times better photooxidation activity toward airborne trichloroethylene compared to the commercial Degussa P25 TiO_2.

Photocatalytic abatement of air NOx also offers an interesting way to remove these harmful gases with high efficiency [202]. Photodecomposition of NOx reactions is diverse and classified into the several methods of photoselective reduction, photo-oxidation, and photodecomposition [203]. Several heterogeneous catalysts based on the metal oxides including V, Cr, Mn, Fe, Co, Ni, Cu, Zn, Y, Zr, Nb, Mo, Ta, and W have been tested as supports for TiO_2 in the photo-deNOx process [204,205]. Despite the strong promises, aerogels utilization in the photo-deNOx process has not been studied much, only a few examples of xerogels out of binary mixed oxides of TiO_2–Al_2O_3 toward the NO oxidation have been reported, so far [206,207].

In photo-oxidation of NO_x, NO convert into NO_3^- on an appropriate photocatalyst according to the following reaction [203]:

$$TiO_2 + h\nu \rightarrow e_{CB}^- + h_{VB}^+ \quad (4)$$

$$h_{VB}^+ + H_2O_{ads} \rightarrow {}^\bullet OH_{ads} + H^+ \quad (5)$$

$$NO + {}^\bullet OH_{ads} \rightarrow HNO_2 \quad (6)$$

$$HNO_2 + {}^\bullet OH_{ads} \rightarrow NO_2 + H_2O \quad (7)$$

$$NO_2 + {}^\bullet OH_{ads} \rightarrow HNO_3 \quad (8)$$

$$NO + {}^\bullet O_2^- \rightarrow NO_3^- \quad (9)$$

$$2NO + {}^\bullet O_2^- + 3e^- \rightarrow 2NO_2 \quad (10)$$

$$3NO_2 + 2OH^- \rightarrow 2NO_3^- + NO + H_2O \quad (11)$$

Soylu et al. [206,207] synthesized mixed oxides of TiO_2–Al_2O_3 through a sol–gel process and after ambient drying and calcination, performed the photooxidation of NO_x over TiO_2–Al_2O_3 surface in order to convert NO to the higher oxidation state of NO_2 and store

it in the solid state in the form of nitrates and nitrites. Their results suggested that alumina can be utilized as active NO_x capturing sites that can eliminate the release of toxic NO_2 into the atmosphere by adsorption as well as storage processes. In fact, the high surface area in Al_2O_3 component enabled both good dispersions of the photocatalytic active TiO_2 domains on the surface as well as the formation of additional storage sites for oxidized NO_x species. Several variables like TiO_2 loading, starting precursors, calcination temperature, and formation of the crystalline phase of TiO_2 have drastically influenced the NO_x photooxidation outcomes [206]. For example, in a molar ratio, Ti/Al = 0.5, better NO_x photocatalytic oxidation (*i.e.* 75% decrease in NO_2 emission, with a high storage performance) than that of commercial TiO_2 and Degussa P25 have been achieved. Also, photocatalytic activity in crystalline forms (anatase and rutile phase) of TiO_2 with which the band gap falls between 3.05 and 3.10 eV has been reported in light of an increased calcination temperature [207].

Polymer, metal oxides, and mixed metal oxide aerogels with their highly porous network structures and good permeability have also been utilized for controlling the indoor and outdoor air quality. These aerogels have been proposed for being used as a suitable air filter or as an air-cleaning device to capture air viral, bacterial bioaerosols, airborne aerosols and respirable particulates [208–212]. In this regard, Kim et al. [208] used hybrid monolithic aerogel of syndiotactic polystyrene (sPS) and polyvinylidene fluoride (PVDF) aerogels for separation of airborne nanoparticles with high filtration efficiency. Guise et al. [213] used packed beds of silica aerogel microspheres and captured aerosols in size range of 20–2000 nm. In some case studies, the airborne bioaerosols were subjected to the deactivation or killing by titanium dioxide through a photocatalysis reaction using a photocatalyst coated on the air filters [214,215] glass plates [216] or using photocatalytic aerogel matrix under ultraviolet (UV) irradiation. Cao [217] synthesized titania–silica aerogel monoliths (Ti/Si = 1) with a high surface area and a good permeability and tested these monoliths for capturing the airborne aerosols and bioaerosols (~0.28 μm) and studied the disinfection capability against *Bacillus subtilis* by taking advantage of photocatalytic oxidation performance of prepared aerogels. The filtration efficiency was reported much better than that of the aerosol filtration test (83% *vs.* 32%) because airborne virus and bacteria usually have larger sizes (>0.3 μm). The subsequent disinfection tests indicated no bacteria colonies/spores observed on most of the agar plates having aerogels.

4. Catalytic applications of aerogels for removal of aqueous pollutants

4.1. Advanced oxidation processes (AOPs)

AOPs refer to the reaction with which the highly reactive species, mainly hydroxyl radicals are produced that can attack the target organic pollutants [218]. In the context of water treatment, aerogels have been considered as an effective heterogeneous catalysis media for decontamination of water through performing different AOP systems such as Fenton, Fenton-like, and ozonation processes. The concept and technical feasibility of AOPs have been explained in detail in several review papers [219,220].

4.1.1. Fenton and Fenton-like processes

The schematic traditional Fenton reaction and its pollutant decomposition activity are sketched in the following reaction scheme:

$$Fe^{2+} + H_2O_2 \rightarrow Fe^{3+} + HO^{\bullet} + HO^{-} \quad (12)$$

$$HO^{\bullet} + \text{organicpollutants} \rightarrow \text{oxidationproducts} \quad (13)$$

In the Fenton process, the catalytic activation of hydrogen peroxide by Fe^{2+} leads to the generation of active $OH^{\bullet}$ radicals that can efficiently degrade organic substances, such as pollutants. The oxidized products sometimes are low molecular weight and biodegradable organic moieties, or quite often carbon dioxide, water, and other inorganics [221]. However, using dissolved iron in the traditional Fenton process has caused a major restriction particularly in the large-scale water decontamination applications due to the need to provide an acidic reaction medium (*e.g.* pH ~ 3) as well as other drawbacks regarding difficulties in catalyst separation and recycling. By using solid heterogeneous catalysts for the activation of H_2O_2, the necessity of having a strict pH control is removed. Also, appropriate design of the catalyst allows the process to act selectively toward the decomposition of a particular type of the contaminant [222,223]. Moreover, most of the heterogeneous catalysts used in this process are prone to the recycling or regeneration process which can be an asset for the economic and cost efficiency of the process. In extensive studies, it has been shown that for the generation of more active iron ion catalysts, it is necessary to disperse (heterogenized) them in a solid inorganic matrix, such as silica, alumina, clay, zeolites, activated carbon, carbon and other solid supports [224–229]. Sol–gel methods and wet impregnation of aqueous iron (III) in the preformed gel have been used in the most of these studies to disperse the iron catalysts on the solid supports. Despite the simplicity, the wet impregnation method has major drawbacks, such as a deficient control in the homogeneity and morphology of iron (III) deposition as well as of the surface area of the resulting catalyst. It has therefore been less exploited compared to the sol–gel approach [230].

Iron oxide and iron supported heterogeneous catalysts have been widely explored for the oxidation of aqueous organic pollutants in the presence of H_2O_2 oxidants. However, a significant improvement in the catalytic performance is expected by preparing these catalysts with a deliberately tailored micro- and a mesoporous structure having an excellent control on pore size, tortuosity and accessible of active centers as well as surface area [230].

Regarding this aim, Li et al. [230] developed a series of high surface area heterogeneous catalysts from Fe/Al binary mixed oxide aerogels and xerogels for water decontamination through a facile propylene oxide-assisted sol–gel approach. The catalytic activity of the prepared aerogel and xerogel materials has been investigated toward the degradation of phenol as a model contaminant and H_2O_2 as the oxidant. It has been shown that tuning the synthesis parameters of binary oxides, such as the ratio of Fe/Al, and the annealing temperature has a major influence on the catalyst activity. The optimum catalytic activities have been obtained at intermediate Fe/Al ratio as the higher Fe loading led to the formation of discrete hematite phases that are known to be catalytically inactive. Also, increasing the catalyst annealing temperature provoked an increase in the pore size of the xerogel and therefore, allowing an easy access of the aqueous reactants to internal pore surface and consequently an improvement in the catalytic activity has been observed.

Carbon materials, especially carbon aerogels which are derived from polymer-based aerogels, have been recognized as promising catalyst support for water purifications due to their rather low cost, high surface area, and readiness in surface modification. Additionally, their simple and straightforward synthesis allows the addition of metal salts easily during synthesis. The metal ions are trapped within the polymer matrix after gelation and in many cases coordinatively bonded to the polymer surface functionalities, *e.g.* by chelating interactions [125]. After carbonization of the polymer aerogel, the metal phase is homogeneously distributed in the porous carbon matrix yielding a metal-doped carbon aerogel catalyst. In order to explore the importance of the catalyst processing methods in the oxidation of water pollutants,

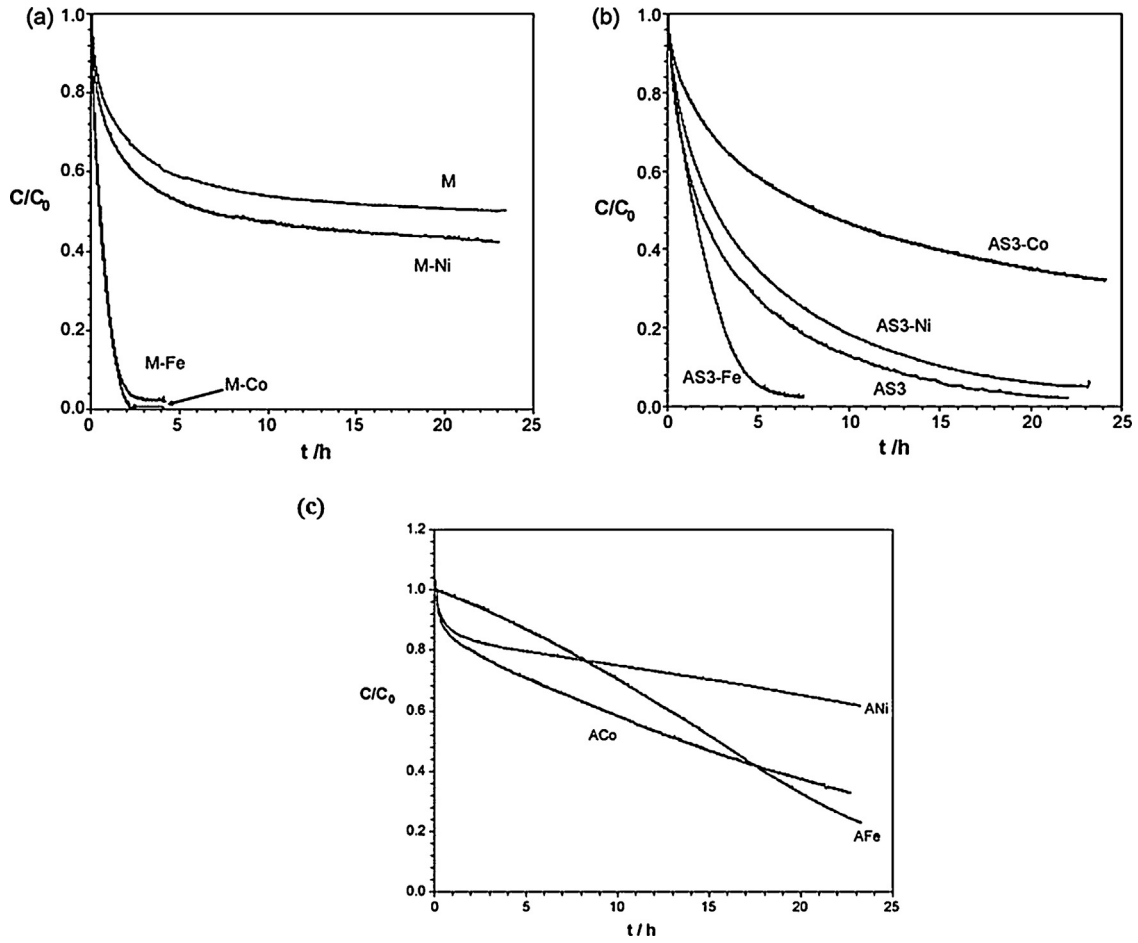

Fig. 9. Orange II elimination catalyzed by M (a), AS3 (b) supports and by the carbon impregnated with Fe, Co, and Ni (T = 30 °C, pH 3, $C_{H_2O_2}$ = 6 mM, C_{cat} = 0.2 g/L), and (c) by doped carbons (T = 30 °C, pH 3, $C_{H_2O_2}$ = 6 mM, C_{cat} = 0.1 g/L). Reprinted with permission from [125].

Ramirez et al. [231] have investigated the role of the support in the catalytic behavior of two different matrices of carbon aerogels (from resorcinol–formaldehyde) and activated carbon (from agricultural products). Both carbon matrices were loaded with Fe (7 wt% loading) through a wet impregnation approach and, have been investigated for a catalytic degradation of non-biodegradable azo-dye Orange II (OII) through a Fenton-like oxidation process. The carbon aerogel showed higher activity in the catalytic degradation of OII compared to the activated carbon, probably due to the homogeneous dispersion of the iron (mainly in Fe (II) oxidation state) on the surface of the aerogel catalyst as well as its appropriate surface chemistry that is rich in the oxygen contents. However, despite the good catalytic performance of this Fe-doped carbon aerogel, leaching of iron species is an important drawback at industrial scales. To diminish the metal losses from the carbon aerogel and to improve the catalytic performance, the same group have utilized two different preparation methods of impregnation and doping approaches to load the carbon aerogel support with several transition metals such as Ni, Fe, Co [125]. In the metal-doping-based approach, corresponding metal precursor (acetates) has been dissolved in initial polymerization solution and after polymerization and carbonization at a temperature of 500 °C, the doped metals acted as an integral part of the global structure of the carbon aerogel matrix with ~3.5% metal loading (A-X, X denoted the metal). In the wet impregnation approach, before the actual impregnation of the carbon aerogels with a metal precursors, the catalyst support has undergone to a carbonization temperature of 500 °C and of 1000 °C for the samples M-X and AS3-X, respectively, followed by an activation of the catalyst in a vapor stream at 900 °C to increase its surface area. Then, both carbon supports were impregnated with an aqueous solution of metal salts, in a final metal content of 7 wt%, and were treated in an inert atmosphere at 300 °C for 2 h. In the case of doped catalysts, ACo and ANi were mesoporous materials with significantly high surface areas, which somewhat induced the adsorption process. However, AFe was macroporous materials with lower surface area and a low leaching rate of metal catalyst.

The catalytic performance of metal doped and impregnated aerogel samples is shown in Fig. 9a–c. In the impregnated samples, M-X, the catalytic activity of the aerogel support for the degradation OII is higher in the presence of Co and Fe (Fig. 9a). Ni has inferior catalytic performances due to its well-known inability in splitting H_2O_2 to $OH^{\bullet}$.

In the case of AS3-Fe (Fig. 9b), the catalytic elimination rate of azo-dye Orange II (OII) has been decreased due to the great extent of adsorption as a result of its high mesopore volume. The inferior catalytic behavior of AS3-Co has been attributed to the greater decrease in the surface area of support upon metal addition as well as the high leaching rate of the metal from the support. The oxidation performance of doped carbon aerogels revealed (Fig. 9c) that the elimination of pollutants in the A–Ni and A–Co were significant at the beginning of reaction due to the adsorption effect as a consequence of the high mesoporous volume and surface area in these samples and then proceeded with catalytic oxidation elimination. While, in the case of A–Fe, due to the greater extent of macroporosity and a lower surface area than A–Co or A–Ni, the OII elimination only proceeded with catalytic degradation as the

higher slope of the curve observed after adsorption process. Nevertheless, Co and Ni were rather catalytically active; Fe has been recognized as the most active metal with the lowest leaching rates in the doped aerogel [125].

Overall, metal-doped carbon aerogels (especially Fe-doped ones) behaved more active as the metal doping approach which could mitigate the metal leaching and sintering effect compared to the metal impregnated catalysts. Although, in this method, metal encapsulation was a drawback and causes a decrease in catalytic behavior as a result of limited contact of the metal with the reactant in the aerogel matrix.

Co-doped carbon aerogels (Co/CA) have been prepared and employed as a heterogeneous catalyst for oxidation of phenol in aqueous solutions by a Fenton-like process [232]. However, instead of using H_2O_2 as an oxidant, sulfate ($SO_4^{-\bullet}$) based oxidants according to Fig. 10a, b have been used which were produced through the reaction of cobalt ions with peroxymonosulfate (oxone) to generate sulfate as well as hydroxyl radicals on the surface of Co/CA catalyst. The generated sulfate radicals decomposed the adsorbed phenol molecules on the aerogel surface to carbon dioxide and water. However, the oxidation of phenol was influenced by other pollutant competitors which were present in the solution such as chlorophenol that has a significant tendency to be adsorbed on the CA catalyst. It has also been claimed that compared to the hydroxyl radicals, sulfate radicals exhibited a higher reactivity and reaction rates toward aqueous organic pollutants because the generation of sulfate radicals from Co^{2+}/oxons is faster than the generation of hydroxyl radicals from Co^{2+}/H_2O_2. Also, degradation of phenol using Co/CA heterogeneous catalyst followed a first order kinetic model with a high dependence on the reaction temperature as a 100% degradation of phenol has been significantly reduced when the temperature increased from 25 to 40 °C (*cf.* Fig. 10c).

4.1.2. Ozonation process

Ozone has also been proposed as another attractive and powerful oxidizing agent that showed a high reactivity toward mineralization of certain aqueous organic pollutants having complex organic molecular structures under specific operational conditions [40].

The reactivity of ozone for decontamination of pollutants is described by two processes: (a) direct reaction of molecular ozone with pollutants and (b) indirect reaction through the generation of hydroxyl radical and subsequent oxidation of contaminants. However, in both ozonation processes, only a partial mineralization of pollutants is observed. Additionally, the low selectivity of the process results in a large portion of OH• radicals to be lost in the aqueous solution and, the high energy demand for ozone generation further limited this process. Using solid catalysts for ozonation processes has drawn significant attention due to the high efficiency in ozone transformations to hydroxyl radicals. Besides, ambient operational conditions in solid catalysts facilitate the ozonation process for real water and wastewater treatment without the additional need for thermal or light energy [233]. In past decades, transition metal oxide catalysts were frequently used as ozonation catalysts [234]. However, major drawbacks associated with using micro- or nanosized metal oxide ozonation catalyst powders are the complication in their separation from wastewaters which in turn causes other issues such as futility in the catalyst regeneration causing secondary pollution especially with iron based homogeneous catalyst, coming into sight [235].

To counteract these drawbacks, one efficient way is again to use heterogeneous catalysts with dispersing the homogenous solid powder (*e.g.* metal oxide) on the matrix of an appropriate support to facilitate the transformation of ozone to hydroxyl radicals [236]. In one way, the high efficiency and ambient operational conditions in heterogeneous catalysts give a potential for practical applications for industrial water treatments. On the other hand, the feasibility of solid catalysts for renewability/recyclability is an asset without imposing further pollutions to water that homogeneous catalysts usually cause.

In recent decades, a wide variety of insoluble heterogeneous catalysts based on dispersed or supported metal oxides, carbon-based materials, zeolites and certain microporous aluminosilicates have emerged [40]. Carbon aerogels, in particular, are attractive catalyst supports for ozonation processes not only for their unique structural and physical features but due to their versatile synthetic chemistry. For the same reasons that are pointed out in Section 4.1.1, carbon aerogels have also been drastically utilized as heterogeneous catalysts in the ozonation process. In fact, the liability for being easily doped with active metal catalysts either in the initial step of the sol–gel reaction by adding metal salts to the monomer solutions or through impregnation of preformed wet gels with a metal salt further affirmed the effectiveness of carbon aerogels for ozonation processes. Ozonation in the surface of carbon aerogels can be performed by direct oxidation of adsorbed aqueous micropollutants with molecular ozone or through the generation of hydroxyl radicals on the aerogel surface and decompose them.

Sanchez-Polo et al. [235] have investigated the efficiency of Co(II)-, Mn(II)-, and Ti(IV)-doped carbon aerogels for the transformation of ozone into OH• radicals for degradation of sodium para-chlorobenzoate (*p*CBA) in drinking water. Despite minimum influences of the metal loadings on the original polymer aerogels' textural and chemical properties, only the Mn-doped carbon aerogel showed a high activity toward the ozonation of (*p*CBA). This is due to the greater rate of ozone transformation into OH• radicals and subsequent oxidation rate of *p*CBA at the surface of Mn-doped carbon aerogels compared to the corresponding Co- and Ti-doped ones. In addition, the capacity of ozone transformation in Mn-doped carbon aerogel was dependent on the used amount of the aerogel catalyst and concentration of Mn(II) on its surface. According to the XPS analysis of Mn-doped carbon aerogels employed in the ozonation treatment of *p*CBA, the transformation of ozone to OH• radicals is proposed to occur following the schematic reaction mechanism indicated below:

$$O_3 + Mn^{2+} \rightarrow MnO^{2+} + O_2 \quad (14)$$

$$MnO^{2+} \rightarrow H_2O \rightarrow MnO^{3+} + OH^{\bullet} + OH^{-} \quad (15)$$

$$2Mn^{3+} + 2H_2O \rightarrow MnO_2 + Mn^{2+} + 4H^{+} \quad (16)$$

In the above reactions, the transformation of ozone to OH• radicals and subsequent degradation of *p*CBA are relying on the oxidation of Mn(II) to Mn(III) and Mn(IV). Apart from the oxidation of Mn(II), the surface chemistry of carbon aerogels is equally important in the acceleration of ozone transformations. The surface activation of carbon aerogels to produce basic groups and to reduce the oxygen species on the surface with an increase in the surface electron density can accelerate the ozone transformation to OH• radicals for an efficient reduction of the organic pollutants.

In another study, nanosized copper oxide catalysts were dispersed in the mesoporous network of carbon aerogels (CuO–Cu_2O/MCA) by sol–gel processing combined with a wet impregnation approach with Cu ions for catalytic ozonation of dyes at simulated wastewaters [236]. The copper oxides were well dispersed in the amorphous structure of carbon aerogels with a size range of 6–14 nm (observed by TEM). The synergetic effect of carbon aerogel supports and copper oxide catalyst provided a durable and effective method for activation of ozone for generation of more hydroxyl radicals and therefore decomposition of dyes. In this study, the degradation efficiency of the catalytic ozonation process has been determined *via* two analytical techniques of color removal or decolorization by recording the absorbance of the dye in the UV–Vis spectrum and COD colorimetry techniques. As

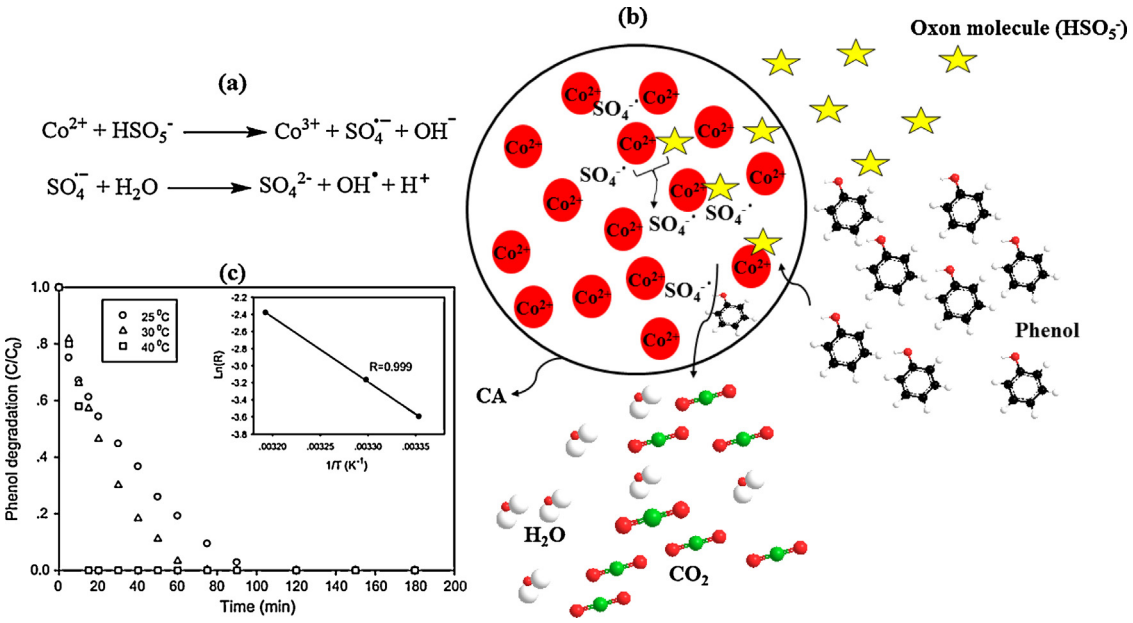

Fig. 10. (a) Reaction mechanism of generation of the sulfate radicals, (b) reaction mechanism of heterogeneous phenol degradation on Co/CA with oxone, (c) effect of temperature on phenol degradation in a heterogeneous system. Reaction conditions: [Phenol] = 50 ppm, Co/CA loading = 0.2 g/L, oxone loading = 2 g/L. Reprinted with permission from Ref. [232].

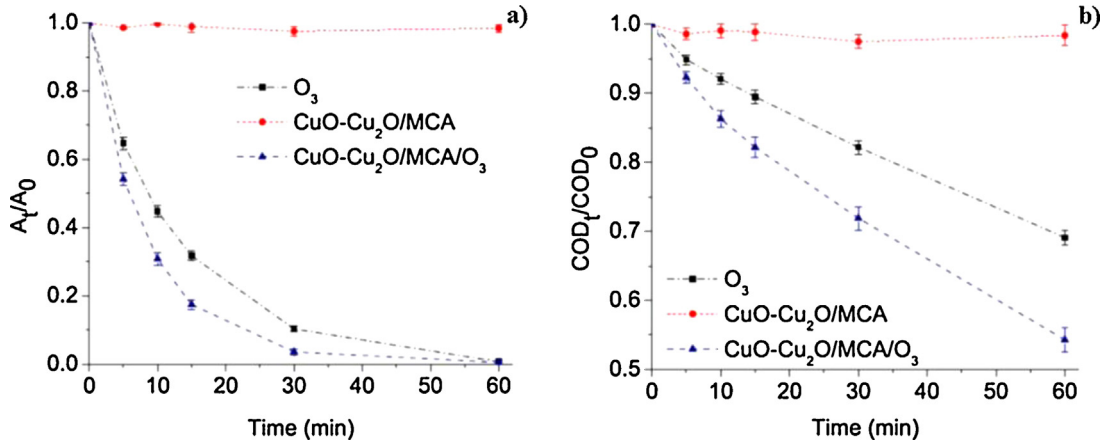

Fig. 11. Comparison of the decolorization (a) and COD removal (b) in different processes. Reaction condition: T = 30 °C; pH = 5.1; ozone dosage = 4.0 mg/min; catalyst dosage = 1 g; $C_{initial}$ RB-5 = 800 mg/L, COD initial = 625 mg/L. The error bars represent the standard deviation of three independent experiments. Reprinted with permission from Ref. [236].

indicated in Fig. 11, it has been shown that CuO–Cu_2O/MCA catalysts have a greater improvement for dye degradations concerning color removal rates than the ozonation process alone (Fig. 11a). Same improvements have occurred regarding COD reduction up to 46% for catalytic ozonation while this value was only 29% for non-catalytic ozonation after 60 min treatment (Fig. 11b). Also, some experimental variables such as increasing the ozone dosage with an enhanced pH value, reaction temperature, and catalyst loading have led to a positive effect on the dye degradation rate regarding both decolorization and COD removal techniques.

4.2. Photocatalysts in water cleaning

Photocatalytic degradation of aqueous phase pollutants is another promising way to deal with the environmental pollution. The photocatalytic degradation of pollutants somehow can be categorized under advanced oxidation processes which are explained above with a small difference in the mechanism. A similar principle compared to the gas phase can be found in the liquid-phase, as well. As shown in below schematic reactions, the light is the source of generation of e^-/h^+ pairs in photocatalytically active phases and, then the subsequent hole in contact with water generated a highly reactive species/radical which are responsible for degradation of pollutants at the catalyst surface.

$$TiO_2 + h\nu \rightarrow TiO_2 + e^- + h^+ \quad (17)$$

$$h^+ + H_2O \rightarrow H^+ + OH^\bullet \quad (18)$$

$$OH^- + h^+ \rightarrow OH^\bullet \quad (19)$$

$$OH^\bullet + \text{Organicpollutant} \rightarrow H_2O + CO_2 \quad (20)$$

Similar to the gas phase, when the commonly used TiO_2 based materials are involved in the aqueous heterogeneous photocatalysis reaction, firstly several properties must be improved. For example, apart from the mitigation of problems regarding the high band gap in TiO_2 which only allows the adsorption of UV light (comprising 5% of solar spectrum), the fast recombination of e^-/h^+

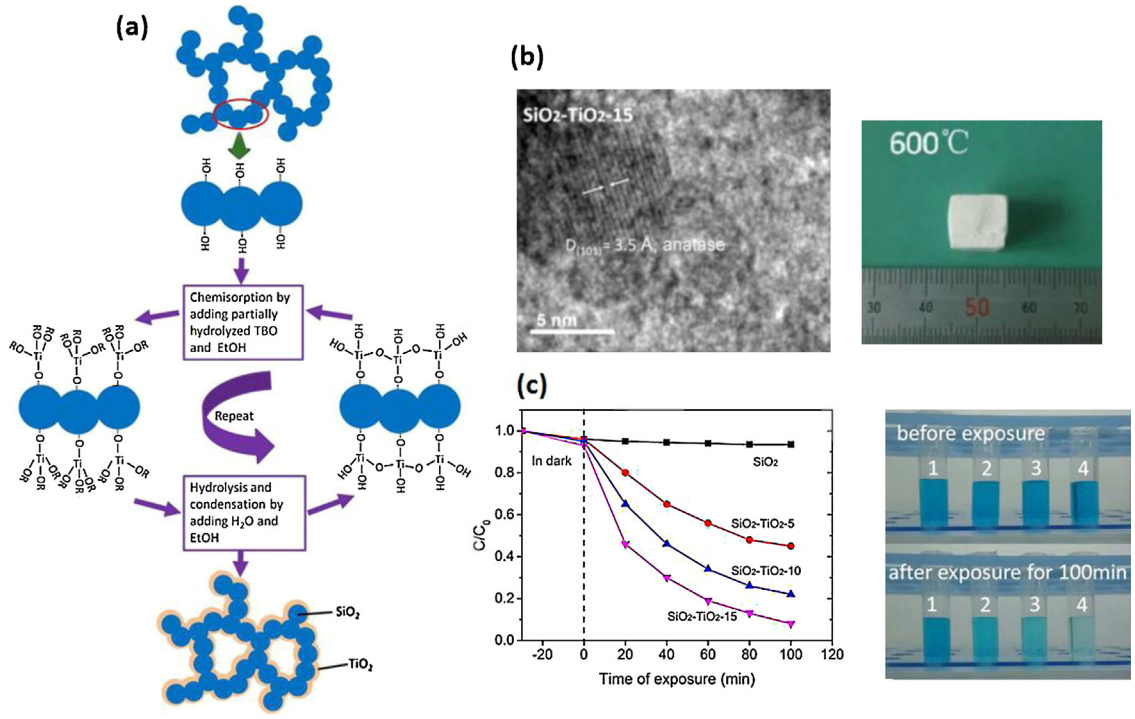

Fig. 12. (a) Schematic representation of preparation of silica–titania composite aerogels *via* a chemical liquid deposition method; (b) photograph of typical aerogels SiO_2-TiO_2-15 treated at 600 °C with its high-resolution TEM micrograph revealing the crystalline anatase phase of TiO_2; (c) changes in MB concentration percentage over the course of the photocatalytic degradation of MB in the presence of the different aerogels after heat treatment at 600 °C along with photographs of MB solution before and after exposure to irradiation for 100 min: (1) MB with silica aerogel, (2) MB with SiO_2-TiO_2-5, (3) MB with SiO_2-TiO_2-10, (4) MB with SiO_2-TiO_2-10. All the aerogels are heat treated at 600 °C for 2 h and have the equal weight. *Note*: SiO_2-TiO_2-5-15 means that the SiO_2–TiO_2 composite was obtained with 5–15 repeated deposition cycles. Reprinted with permission from Ref. [259].

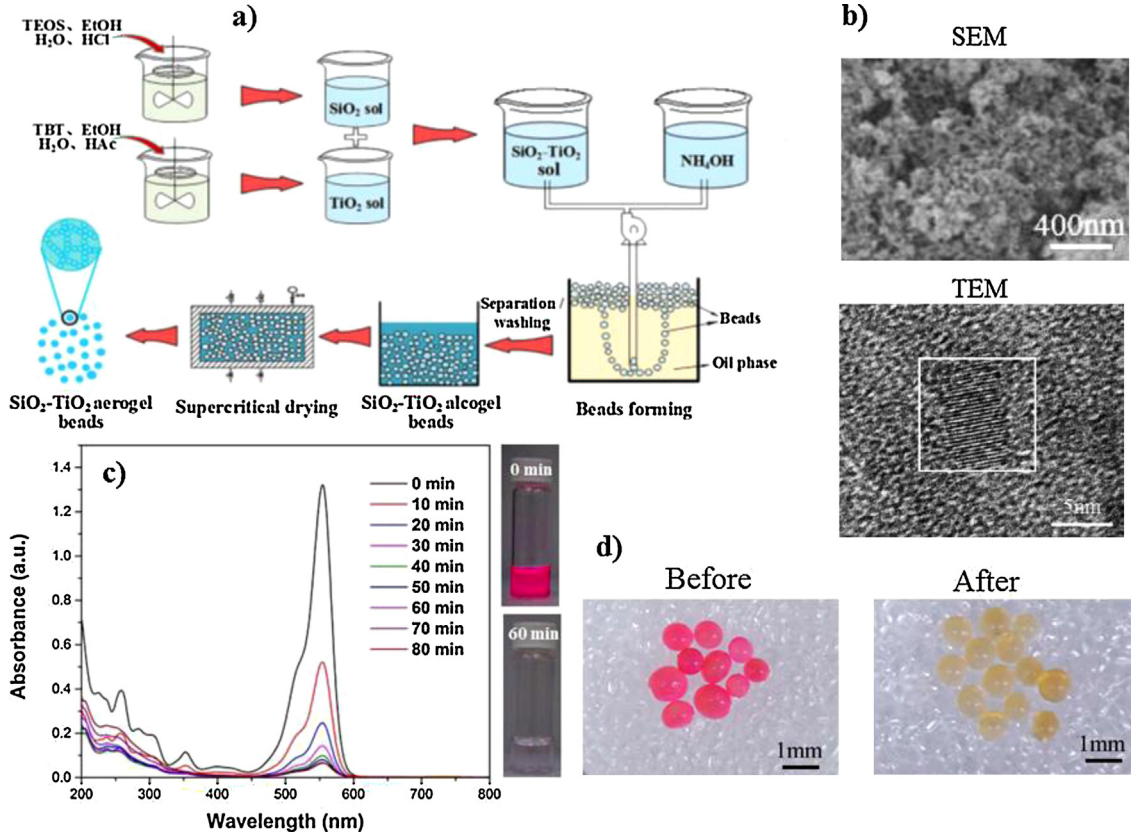

Fig. 13. (a) The schematic representation of the synthesis process of SiO_2–TiO_2 aerogel beads, (b) SEM and TEM micrographs of SiO_2–TiO_2 aerogel beads, (c) time-dependent UV–vis absorption spectra of RhB solution with SiO_2–TiO_2 aerogel beads (Si-Ti-5). The inset is the photographs of RhB solution before, and after the addition of SiO_2–TiO_2 aerogel beads, (d) photographs of RhB adsorbed SiO_2–TiO_2 aerogel beads before and after 30 min UV irradiation. Reprinted with permission from Ref. [254].

Table 3
Selected list of aerogel photocatalyst for depollution of aqueous systems.

Aerogel photocatalysts	Synthesis	Properties/remarks	Ref.
Gold nanoparticles (Au NPs) loaded titania (Au/TiO_2)	The wet gel of TiO_2 obtained from the sol–gel process was impregnated with Au colloidal solution with the size of 4–10 nm.	• Au nanoparticle (NPs) sizes and concentration affected the morphostructural and crystallinity of resulted aerogels. • Au NPs led to increase in the crystalline zone in titania. • The higher the concentration of gold NPs, the more photodegradation of salicylic acid under UV light was obtained.	[252]
BiOBr/reduced graphene oxide (RGO) composite	A one-pot hydrothermal method using L-lysine as a reducing agent and the cross-linker was applied to prepare three-dimensional RGO-based porous network with simultaneous growing BiOBr nanoparticles in its network.	• Excellent dye degradation performance BiOBr under visible light due to charge separation effect of RGO • High surface area with spongy nature • High stability and recyclability from aqueous solutions	[240]
Titania–silica microspheres (TSAMs)	A one-pot sol–gel processes in water in oil microemulsion system followed by an ambient pressure drying approach were employed to prepare aerogel microspheres.	• TSAMs contained mean diameters of about 100 μm, a specific surface area of 415 $m^2\ g^{-1}$. • A better photocatalytic activity and recyclability than P25 TiO_2 for degradation of MB was achieved.	[265]
Nanocrystalline TiO_2	An epoxide mediated sol–gel synthesis followed by super and subcritical dryings with calcination process at 400–700 °C	• Nanocrystalline TiO_2 aerogels calcined at 650 °C has shown a superior photodegradation ability for aqueous phenol. • The photocatalytic activity was correlated with nanocrystalline phase and crystalline sizes.	[191]
Binary titania–silica (TiO_2–SiO_2)	A one pot sol–gel reaction by using $TiOCl_2$ and sodium silicate as precursors	• Aerogel has hydrophobic properties. • Increasing the calcination temperature up to 400 °C increased the surface area. • Photodegradation ability of aerogels toward (MB) were correlated with their morphostructural and hydrophobic properties as well as calcination temperature.	[266]
Europium oxide doped TiO_2 (Eu-TiO_2)	Europium oxide was doped conveniently to titania by sol–gel approach	• An improved photocatalytic performance toward degradation of salicylic acid was achieved due to (1) the prolonged separation of electrons and holes which were facilitated by the formation of defects (Ti^{3+}) and oxygen vacancies on the surface, (2) the ability of europium ions to trap electrons and minimize charge carrier recombination under UV irradiation, (3) presence of photoactive anatase crystalline phase.	[251]
Nanoglued binary titania–silica (TiO_2–SiO_2)	A preformed titania with an anatase phase was immobilized on a 3D mesoporous network of silica obtained from sol–gel.	• Aerogels contained a high-surface-area with a Ti^{4+} valency. • The photogenerated hydroxyl radicals ($OH^{\bullet}$) in the solution were responsible for the oxidation of MB. • The photocatalytic reaction has followed a pseudo first-order Langmuir–Hinshelwood (L–H) kinetic model.	[267]
$CeVO_4$/graphene composite	Aerogels were prepared by an electrostatic-driven self-assembly method.	• $CeVO_4$ particles were anchored uniformly on the flexible graphene sheets. • The light absorption capability of composite improved with an effective charge transfer from $CeVO_4$ particles to graphene which led to increasing in the photodegradation ability of composites toward MB. • The chemical structure of composites was stable during several cyclic reactions.	[268]
Cu_2O/RGO composite	Aerogels were synthesized through a facile one-pot hydrothermal method using glucose as a reducing agent and cross-linker.	• Aerogels were employed for aqueous methyl orange photodegradation. • Enhanced light absorption capability as a result of improved charge separation ability of composite by RGO was achieved. • Easy recycling due to the aerogel's light weight and hydrophobicity was obtained.	[243]
SiO_2–SnO_2 composite	Tine oxide was deposited on preformed silica gel through a wet deposition approach.	• Crystallinity and grain size of SnO_2 increased with thermal treatment at >500 °C that caused an improved photocatalytic activity. • Aerogel exhibited rich photoluminesce effects as a result of defects especially for those related to the oxygen-deficient sites. • Aerogel composite has a proven photodegradation performance for decomposition of MB.	[269]
N-doped TiO_2 syndiotactic polystyrene nanocomposite (Nt-sPS)	The N-doped-TiO_2 obtained by a nitration process during hydrolysis of titanium alkoxide and then deposited on the syndiotactic polystyrene network.	• The syndiotactic polystyrene support offers a high surface area, low density, and monolithic to the composites. • Photocatalytic activity toward MB under visible light was achieved. • A better photocatalytic activity and recovering ability were achieved in compared to the N-doped-TiO_2 in powdered forms.	[270]
TiO_2-Ca alginate polymer fibers composite	The composite was obtained by dispersion of TiO_2 in the hollow alginate fiber matrix through a chemical vapor deposition method.	• High porosity and surface area were achieved for composite compared to their non-porous fiber counterparts • The photodegradation toward MO for composite was much higher (three-fold enhancement) than that of non-porous fiber counterparts as well as TiO_2 powder. • The method of composite development is easily upscalable.	[249]

pairs, the morphostructural properties such as specific surface area, porosity, and crystallinity as well as surface hydrophobicity of photocatalyst are highly influential factors in the liquid phase photodegradation process.

Current research efforts are focused on the preparation of more efficient and diverse photocatalysts with a better photoactivity having a narrow band gap with high response to visible light and good separation of e^-/h^+ pairs for detoxification of water from widespread pollutants [237]. Also, for practical applications of semiconductor photocatalysts in water purification, it is ideal to immobilize the nanostructured photocatalyst on a solid surface for easy recycling and recovering [238,239]. The ideal solid sup-

port should have a large specific surface area, open pores with high interconnectivity for mass transport, and appropriate surface functionalities to anchor the photoactive phases [237]. In general, aerogels are ideal photocatalytic supports due to their peculiar properties such as large specific surface area, open porous structure, and tunable surface chemistry that make them appealing as a support for semiconductor photocatalysts [240]. More than these, the lightweight and controlled hydrophobicity in aerogel supports make them capable of floating on the water surface that not only allows them to absorb more solar radiation but also facilitate their recovery and recycling without being lost during the repeated cycles.

In principle two approaches can be followed: (a) the semiconductor itself can be processed into a highly porous 3D aerogel network (*e.g.* TiO_2 aerogels) or (b) semiconducting nanostructures can be deposited on another inactive aerogel support *via* impregnation of one-pot sol–gel approaches. The wet chemical synthesis is always followed by a high-temperature supercritical drying or thermal treatment. In this case, the sol–gel process allows the molecular to the nano-level mixing of photoactive, semiconducting elements with the support and also allows to tailor the network from nano to micrometer lengths scale [241].

Although nowadays various types of aerogel supports from biomass derived carbon aerogels, graphene, to polysaccharide-based aerogels are being emerged [241–250], the majority of studies in the photocatalytic water purification applications of aerogels are devoted to titania aerogels and their composites with other semiconductor elements [251–253]. In addition, binary silica–titania aerogels are of interest. Using the binary silica–titania aerogels is advantageous as this composite combines the large surface area/porosity with the high adsorption capability of silica aerogels with the semiconductor behavior of TiO_2 to yield a high-performance heterogeneous photocatalyst [254]. However, still, the challenge in this area is to improve the aerogel properties by controlling the manifold synthesis and processing conditions in order to establish a well-understood structure–property relationship. For example, Ahmed and Attia [255] prepared silica–titania binary photocatalyst aerogels for photodegradation of aqueous cyanide into CO_2 and N_2. They have found that the high content of SiO_2 increased the photodegradation efficiency as the presence of SiO_2 decreased the extent of shrinkage during drying and generated high specific surface area, translucent and crack free aerogel monolith which can easily be handled and recycled several times and absorbed light efficiently. In contrast, in the study by Deng et al. [256], the best photocatalytic activity of TiO_2–SiO_2 has been achieved at a molar ratio Ti:Si = 1:1. Above this molar ratio, the higher the content of SiO_2, the less efficient photodegradation of phenol was, which might be due to the fact that the high contents of SiO_2 do not allow the easy access of pollutants to the photoactive sites. In the study by Malinowska et al. [196] the photocatalytic activity of both pure TiO_2 and TiO_2-SiO_2 aerogels toward different phenol para-derivatives (p-chlorophenol, p-nitrophenol, 4-hydroxybenzoic acid) were explored. The photocatalytic activity of pure titania aerogels was much better than that of binary aerogels due to the occurrence of phase separation between two phases and less likely of the creation of chemical linkage of Si—O—Ti. However, Gao et al. [257] suggested a better photocatalytic activity for binary silica–titania aerogels than that of pure titania aerogels which was ascribed for the charge transfer behavior of SiO_2 that can rapidly transfer the photoinduced electrons and holes to the solution and, to the network ligands and inhibits their fast recombination.

Zhu et al. [258] developed ambient pressure dried, recyclable superhydrophobic silica–titania aerogels for the adsorption and photocatalytic decomposition of Rhodamine B (Rh-B), a toxic organic dye, from the water. These binary aerogels show a photodegradation capability for decomposition of more than 75% of Rh-B within 100 min of exposing to UV light. Moreover, the hydrophobicity of these binary aerogels has been an essential property which not only allows the aerogel to float on water which facilitates capturing the pollutants and accumulating them in the vicinity of active TiO_2 sites, but it also allows the effective capturing the UV light without losing the surface hydrophobicity.

Silica–titania aerogels have also recently been reported through chemical liquid deposition (in a repeated deposition cycle 5–15) of prehydrolyzed titanium alkoxides (10–20 wt%) on the preformed silica wet gels by reaction of hydroxyl groups on the silica network with those on the partially hydrolyzed titania in water (*cf.* Fig. 12a) [259]. After heat treatment at 600 °C, the typical obtained composite aerogel after 15 deposition cycles (SiO_2-TiO_2-15) possessed a surface area of 425 $m^2\,g^{-1}$ which were suitable for effective catalytic degradation of methylene blue (MB) in water. As a result of repeated deposition, the growth of titania nanoparticles and titania nanocoating on silica surface have been occurred and led to the formation of silica–titania composite aerogels. Apart from the surface area in composite, the small particle size and crystallinity in titania, as well as deposition cycle, have significantly influenced the photocatalytic performance of composites. Formation of anatase TiO_2 phase has been tracked by using a high-resolution TEM and with observing the clear lattice fringes corresponding to (101) planes (*cf.* Fig. 12b). As shown in Fig. 12c, after exposure for 100 min, the concentration percentages of MB with sample SiO_2-TiO_2-5, SiO_2-TiO_2-10 and SiO_2-TiO_2-15 were 45%, 22%, and 8% respectively [259].

Recyclable silica–titania aerogel photocatalyst beads were also prepared through a simple synthesis approach as indicated in Fig. 13a for degradation of Rh-B in the water [254]. The synthesis method involved the co-condensation of titanium and silicon alkoxides in varied Ti/Si molar ratios. The resulting sol was extruded through a nozzle into an oil phase to rapidly get into an alcogel which after washing was dried by high temperature supercritical extraction.

Fig. 13b shows the interconnected porous structure of TiO_2–SiO_2 aerogel beads in which the titania anatase crystalline phase is uniformly distributed in the silica network. Rh-B has a maximum UV absorbance at 554 nm, which decreases over time when being adsorbed by the aerogel beads and removed from the water upon photocatalytic degradations (Fig. 13c). Approximately 80% of Rh-B was removed within 20 min of exposure to TiO_2–SiO_2 aerogel beads. Moreover, after 30 min of UV light irradiation, the color of Rh-B adsorbed on these aerogels faded away and changed to the yellow, thus indicating an excellent photocatalytic performance of the aerogels beads (Fig. 13d).

Ismail and Ibrahim [260] have studied the impact of supercritical drying and heat treatment on physical and the photodegradation properties of silica–titania aerogels for the purification of industrial waste streams containing Cl^-, S^{2-}, NH_4^+ and traces of heavy metal ions. The best aerogels regarding the photodegradation capabilities have been obtained when they were processed by high-temperature supercritical drying for 30 min period along with 5 h heat treatment. These processing steps were necessary for the evolution of photoactive anatase crystalline phase of titania on the aerogel structure.

Carbon based TiO_2 composites are also one of the most extensively studied photocatalysts in waste water treatments. Carbon-TiO_2 composites exist in three different structures of a TiO_2-C hybrid; carbon supported, carbon doped and carbon coated TiO_2 [261], from which many different beneficial characteristics have been achieved. The cationic and anionic doping of TiO_2 with carbon [262,263] is reported to narrow its band gap and enhance its photocatalytic activity in the visible range. The nanocomposite of TiO_2 and other semiconductors with carbon allotropes, such as carbon nanotubes and graphene [240,264], are also reported to

decrease the e^-/h^+ pairs recombination, reduce the band gap and increase the pollutant absorptivity.

The one pot synthesis of C-TiO_2 hybrid aerogel with macroporous structures (pore size up to ~996 nm) and better photocatalytic properties (4.23 time) than that of the P25, a commercial TiO_2 (Degussa Co., Ltd., Germany), toward degradation of methylene blue under UV light has been reported [241]. The high catalytic activity has been attributed to the large light absorption capability of the hybrid aerogel as a result of light scattering and the presence of oxygen vacancy at anatase phase TiO_2 nanoparticles. In fact, carbon aerogels inhibit TiO_2 nanoparticles' growth and increase the crystallinity of TiO_2 during heat treatment and suppress the TiO_2 phase transformation from photoactive anatase phase to the less photoactive rutile phase.

The photocatalytic activity of various aerogels reported in the literature for pollution abatement of aqueous systems is compiled and summarized in Table 3.

5. Conclusions and outlooks

This paper constitutes the first review article in last ten years which exclusively reviews the catalytic and photocatalytic environmental pollution abatement using various aerogel and aerogel supported catalysts. The literature studied in here is indicating the increasing interest over the last few years in applications of aerogels as (photo)catalysts or (photo)catalytic supports for depollution of air and water media.

Based on the literature summarized in the present paper, aerogels are promising candidates for being used as a catalytic abatement media for environmental pollutants due to their versatile synthesis chemistry, the solution-based sol–gel process, accompanied with supercritical drying which would allow the tailoring the material's physico-chemical, textural and morphostructural properties for different catalytic reactions. A drastic enhancement in catalytic activity, selectivity, and stability can be attributed to the combination of the aerogels exclusive physical properties like high specific surface areas accessible to reactant/product molecules, high dispersion of active species, and strong metal or catalyst-support or metal–metal interactions. Also, thanks to the high and homogeneous dispersion of (photo)catalytic active phases on aerogel supports, the aggregation problem of nanoscale catalysts as a result of their high surface to volume ratio are mitigated and therefore a better (photo)catalytic activity can be achieved with aerogels.

Although the current review paper only focuses on the environmental cleaning applications of aerogel catalysts, this fascinating class of materials has also shown fruitful performances in steam reforming processes for producing hydrogen as a clean energy source for onboard, on-demand applications as well as chemical product synthesis. However, despite the fact that the catalytic applications of aerogels are potentially immense in number and huge in impact, they are not currently commercially available due to the rather expensive processing as well as the presence of other bottlenecks like low thermal resistance and delicate mechanical strength.

In order to pave the way for large-scale productions and applications, today, these issues are being mitigated to some extent by using, for example, cheap inorganic salts instead of their expensive alkoxide counterparts or using sustainable biomass derived sources as precursors. Moreover, safe aerogel processing techniques *i.e.* replacing the supercritical CO_2 extraction with an ambient pressure drying approach as well as taking profit of hybridization chemistry to constitute aerogel catalysts with better mechanical and thermal performance can counter balance these limitations for future applications.

Acknowledgement

Hajar Maleki acknowledges financial support by the Austrian Science Fund, FWF, for the Lise Meitner fellowship (project number: M2086-N34).

References

[1] N. Hüsing, U. Schubert, Aerogels—airy materials: chemistry, structure, and properties, Angew. Chem. Int. 37 (1998) 22–45.
[2] H. Maleki, Recent advances in aerogels for environmental remediation applications, Chem. Eng. J. 300 (2016) 98–118.
[3] H. Maleki, L. Durães, C.A. García-González, P. del Gaudio, A. Portugal, M. Mahmoudi, Synthesis and biomedical applications of aerogels: possibilities and challenges, Adv. Colloid Interface Sci. 36 (2016) 1–27.
[4] M. Koebel, A. Rigacci, P. Achard, Aerogel-based thermal superinsulation: an overview, J. Sol–Gel Sci. Technol. 63 (2012) 315–339.
[5] R. Baetens, B.P. Jelle, A. Gustavsen, Aerogel insulation for building applications: a state-of-the-art review, Energy Build. 43 (2011) 761–769.
[6] G.M. Pajonk, Some catalytic applications of aerogels for environmental purposes, Catal. Today 52 (1999) 3–13.
[7] J. Choi, D.J. Suh, Catalytic applications of aerogels, Catal. Surv. Asia 11 (2007) 123–133.
[8] S.S. Kistler, Coherent expanded aerogels and jellies, Nature 127 (1931) 741.
[9] H. Maleki, L. Duraes, A. Portugal, An overview on silica aerogels synthesis and different mechanical reinforcing strategies, J. Non-Cryst. Solids 385 (2014) 55–74.
[10] S.S. Kistler, S.J. Swann, E.G. Appel, Aerogel catalysts – thoria: preparation of catalyst and conversions of organic acids to ketones, Ind. Eng. Chem. 26 (1934) 388–391.
[11] G.M. Pajonk, S.J. Tichner, in: J. Fricke (Ed.), Proceedings of the First International Symposium on Aerogels, Wurzburg, Germany, 1985, pp. 23–25.
[12] G.M. Pajonk, Aerogel catalysts, Appl. Catal. 72 (1991) 217–266.
[13] G.M. Pajonk, Catalytic aerogels, Catal. Today 35 (1997) 319–337.
[14] R. Tleimat-Manzalji, T. Manzalji, G.M. Pajonk, Aerogels and xerogels for catalytic applications, J. Non-Cryst. Solids 147&148 (1992) 744–747.
[15] C. Moreno-Castilla, F.J. Maldonado-Hodar, Carbon aerogels for catalysis applications: an overview, Carbon 43 (2005) 455–465.
[16] M. Schneider, A. Baiker, Aerogels in catalysis, Catal. Rev. Sci. Eng. 37 (1995) 515–556.
[17] J.E. Amonette, J. Matyáš, Functionalized silica aerogels for gas-phase purification, sensing, and catalysis: a review, Microporous Mesoporous Mater. (2017).
[18] B.C. Dunn, P. Cole, D. Covington, M.C. Webster, R.J. Pugmire, R.D. Ernst, E.M. Eyring, N. Shah, G.P. Huffman, Silica aerogel supported catalysts for Fischer–Tropsch synthesis, Appl. Catal. A: Gen. 278 (2005) 233–238.
[19] S. Bali, F.E. Huggins, G.P. Huffman, R.D. Ernst, R.J. Pugmire, E.M. Eyring, Iron aerogel and xerogel catalysts for Fischer–Tropsch synthesis of diesel fuel, Energy Fuels 23 (2009) 14–18.
[20] D.J. Suh, Catalytic applications of composite aerogels, J. Non-Cryst. Solids 350 (2004) 314–319.
[21] M. Power, B. Hosticka, E. Black, C. Daitch, P. Norris, Aerogel as biosensors: viral particle detection by bacteria immobilized on large pore aerogel, J. Non-Cryst. Solids 285 (2001) 303–308.
[22] P. Buisson, C. Hernandez, M. Pierre, A. Pierre, Encapsulation of lipases in aerogels, J. Non-Cryst. Solids 285 (2001) 295–302.
[23] M.R. Ayers, A.J. Hunt, Molecular oxygen sensors based on photoluminescent silica aerogels, J. Non-Cryst. Solids 225 (1998) 343–347.
[24] Y.K. Li, Y.-C. Chen, K.-J. Jiang, J.-C. Wu, Y.W. Chen-Yang, Three-dimensional arrayed amino aerogel biochips for molecular recognition of antigens, Biomaterials 32 (2011) 7347–7354.
[25] J.A. Cusumano, Environmentally sustainable growth in the 21st century: the role of catalytic science in technology, J. Chem. Educ. 72 (1995) 959.
[26] H. Rotter, M.V. Landau, M. Carrera, D. Goldfarb, M. Herskowitz, High surface area chromia aerogel efficient catalyst and catalyst support for ethylacetate combustion, Appl. Catal. B: Environ. 47 (2004) 111–126.
[27] M.A. Reiche, E. Ortelli, A. Baiker, Vanadia grafted on TiO_2–SiO_2, TiO_2 and SiO_2 aerogels structural properties and catalytic behaviour in selective reduction of NO by NH_3, Appl. Catal. B: Environ. 23 (1999) 187–203.
[28] H. Bosch, F. Janssen, Formation and control of nitrogen oxides, Catal. Today 2 (1988) 369–532.
[29] J.N. Armor, Environmental catalysis, Appl. Catal. B 1 (1992) 221–256.
[30] G. Busca, L. Liettib, G. Ramis, F. Berti, Chemical and mechanistic aspects of the selective catalytic reduction of NOx by ammonia over oxide catalysts: a review, Appl. Catal. B: Environ. 18 (1998) 1–36.
[31] X. Cheng, X.T. Bi, A review of recent advances in selective catalytic NOx reduction reactor technologies, Particuology 16 (2014) 1–18.
[32] B. Guan, R. Zhan, H. Lin, Z. Huang, Review of state of the art technologies of selective catalytic reduction of NOx from diesel engine exhaust, Appl. Therm. Eng. 66 (2014) 395–414.
[33] L. Zhiming, H. Jiming, F. Lixin, L. Junhua, C. Xiangyu, Advances in catalytic removal of NOx under lean-burn conditions, Chin. Sci. Bull. 49 (2004) 2231–2241.

[34] R.J. Farrauto, C.H. Bartholomew, Fundamentals of Industrial Catalytic Processes, Blackie Academic, London, 1997, pp. 640–645.
[35] H. Chen, C.E. Nanayakkara, V.H. Grassian, Titanium dioxide photocatalysis in atmospheric chemistry, Chem. Rev. 112 (2012) 5919–5948.
[36] S. Kwon, M. Fan, A.T. Cooper, H. Yang, Photocatalytic applications of micro- and nano-TiO_2 in environmental engineering, Crit. Rev. Environ. Sci. Technol. 38 (2008) 197–226.
[37] S.W. Yao, H.P. Kuo, Photocatalytic degradation of toluene on SiO_2/TiO_2 photocatalyst in a fluidized bed reactor, Procedia Engineering (The 7th World Congress on Particle Technology (WCPT7)), vol. 102 (2015) 1254–1260.
[38] S. Cao, H. Zhang, Y. Song, J. Zhang, H. Yang, L. Jiang, Y. Dan, Investigation of polypyrrole/polyvinyl alcohol-titanium dioxide composite films for photo-catalytic applications, Appl. Surf. Sci. 342 (2015) 55–63.
[39] L. Qie, W.M. Chen, H.H. Xu, X.Q. Xiong, Y. Jiang, F. Zou, X.L. Hu, Y. Xin, Z.L. Zhang, Y.H. Huang, Synthesis of functionalized 3D hierarchical porous carbon for high-performance supercapacitors, Energy Environ. Sci. 6 (2013) 2497–2504.
[40] D. Shahidi, R. Roy, A. Azzouz, Advances in catalytic oxidation of organic pollutants – prospects for thorough mineralization by natural clay catalysts, Appl. Catal. B: Environ. 174–175 (2015) 277–292.
[41] M. Niederberger, N. Pinna, Aqueous and Nonaqueous Sol–Gel Chemistry, Metal Oxide Nanoparticles in Organic Solvents: Synthesis, Formation, Assembly and Application, Springer, 2009.
[42] A. Feinle, M.S. Elsaesser, N. Hüsing, et al., Hierarchical organization in monolithic sol–gel materials, in: K. Lisa (Ed.), Handbook of Sol–Gel Science and Technology, Springer International Publishing Switzerland, 2016.
[43] P.H. Mutin, A. Vioux, Recent advances in the synthesis of inorganic materials via non-hydrolytic condensation and related low temperature routes, J. Mater. Chem. A 1 (2013) 11504–11512.
[44] R.W. Pekala, Organic aerogels from the polycondensation of resorcinol with formaldehyde, J. Mat. Sci. 24 (2017) 3221–3227.
[45] A. Feinle, M.S. Elsaesser, N. Hüsing, Sol–gel synthesis of monolithic materials with hierarchical porosity, Chem. Soc. Rev. 45 (2016) 3377–3399.
[46] C.A. García-González, M. Alnaief, I. Smirnova, Polysaccharide-based aerogels—promising biodegradable carriers for drug delivery systems, Carbohydr. Polym. 86 (2011) 1425–1438.
[47] F. Quignard, R. Valentin, F. Di Renzo, Aerogel materials from marine polysaccharides, New J. Chem. 32 (2008) 1300–1310.
[48] J.A. Schwarz, C. Contescu, A. Contescu, Methods for preparation of catalytic materials, Chem. Rev. 95 (1995) 477–510.
[49] D.R. Rolison, Catalytic nanoarchitectures – the importance of nothing and the unimportance of periodicity, Science 299 (2003) 1698–1701.
[50] T.F. Baumann, A.E. Gash, G.A. Fox, J.H. Satcher Jr., L.W. Hrubesh, Handbook of Porous Solids, Wiley-VCH, Weinheim, 2002.
[51] A. Feinle, N. Husing, Mixed metal oxide aerogels from tailor-made precursors, J. Supercrit. Fluids 106 (2015) 2–8.
[52] C. Beck, T. Mallat, T. Bürgi, A. Baiker, Nature of active sites in sol–gel TiO_2–SiO_2 epoxidation catalysts, J. Catal. 204 (2001) 428–439.
[53] J.B. Miller, S.E. Rankin, E.I. Ko, Strategies in controlling the homogeneity of zirconia–silica aerogels: effect of preparation on textural and catalytic properties, J. Catal. 148 (1994) 673–682.
[54] B.J. Clapsaddle, A.E. Gash, J.H. Satcher, R.L. Simpson, Silicon oxide in an iron(III) oxide matrix: the sol–gel synthesis and characterization of Fe–Si mixed oxide nanocomposites that contain iron oxide as the major phase, J. Non-Cryst. Solids 331 (2003) 190–201.
[55] M. Schneider, U. Scharf, A. Wokaun, A. Baiker, Vanadia–titania aerogels: III. Influence of niobia on structure and activity for the selective catalytic reduction of NO by NH_3, J. Catal. 150 (1994) 284–300.
[56] J. Wang, S. Uma, K.J. Klabunde, Visible light photocatalytic activities of transition metal oxide/silica aerogels, Microporous Mesoporous Mater. 75 (2004) 143–147.
[57] A. Corrias, M.F. Casula, Aerogels containing metal, alloy, and oxide nanoparticles embedded into dielectric matrices, in: M.A. Aegerter, N. Leventis, M. Koebel (Eds.), Aerogels Handbook, Springer, New York, 2011, pp. 355–363.
[58] C.J. Brinker, G.W. Scherer, Sol–Gel Science, Academic Press, New York, 1990.
[59] D.M. Smith, D. Stein, J.M. Anderson, W. Ackerman, Preparation of low-density xerogels at ambient pressure, J. Non-Cryst. Solids 186 (1995) 104–112.
[60] H. Maleki, L. Durães, A. Portugal, Development of mechanically strong ambient pressure dried silica aerogels with optimized properties, J. Phys. Chem. C 119 (2015) 7689–7703.
[61] R.W. Pekala, Organic aerogels from the polycondensation of resorcinol with formaldehyde, J. Mater. Sci. 24 (1989) 3221–3227.
[62] H. Maleki, L. Duraes, B.F.O. Costa, R.F. Santos, A. Portugal, Design of multifunctional magnetic hybrid silica aerogels with improved properties, Microporous Mesoporous Mater. 232 (2016) 227–237.
[63] D. Nadargi, J. Gurav, M.A. Marioni, S. Romer, S. Matam, M.M. Koebel, Methyltrimethoxysilane (MTMS)-based silica–iron oxide superhydrophobic nanocomposites, J. Colloid Interface Sci. 459 (2015) 123–126.
[64] J.L. Mohanan, I.U. Arachchige, S.L. Brock, Porous semiconductor chalcogenide aerogels, Science 307 (2005) 397–400.
[65] I.U. Arachchige, S.L. Brock, Sol–gel methods for the assembly of metal chalcogenide quantum dots, Acc. Chem. Res. 40 (2007) 801–809.
[66] N. Leventis, N. Chandrasekaran, C. Sotiriou-Leventis, A. Mumtaz, Smelting in the age of nano: iron aerogels, J. Mater. Chem. 19 (2009) 63–65.
[67] N. Leventis, N. Chandrasekaran, A.G. Sadekar, S. Mulik, C. Sotiriou-Leventis, The effect of compactness on the carbothermal conversion of interpenetrating metal oxide/resorcinol–formaldehyde nanoparticle networks to porous metals and carbides, J. Mater. Chem. 20 (2010) 7456–7471.
[68] S. Mahadik-Khanolkar, S. Donthula, A.W.C. Bang, C. Sotiriou-Leventis, N. Leventis, Polybenzoxazine aerogels. 2. Interpenetrating networks with iron oxide and the carbothermal synthesis of highly porous monolithic pure iron(0) aerogels as energetic materials, Chem. Mater. 26 (2014) 1318–1331.
[69] W. Liu, A.-K. Herrmann, N.C. Bigall, P. Rodriguez, D. Wen, M. Oezaslan, T.J. Schmidt, N. Gaponik, A. Eychmüller, Noble metal aerogels – synthesis, characterization, and application as electrocatalysts, Acc. Chem. Res. 48 (2015) 154–162.
[70] W. Liu, A.-K. Herrmann, D. Geiger, L. Borchardt, F. Simon, S. Kaskel, N. Gaponik, A. Eychmüller, High-performance electrocatalysis on palladium aerogels, Angew. Chem. Int. Ed. 51 (2012) 5743–5747.
[71] A.-K. Herrmann, P. Formanek, L. Borchardt, M. Klose, L. Giebeler, J. Eckert, S. Kaskel, N. Gaponik, A. Eychmüller, Multimetallic aerogels by template-free self-assembly of Au, Ag, Pt, and Pd nanoparticles, Chem. Mater. 26 (2014) 1074–1083.
[72] N. Gaponik, A.-K. Herrmann, A. Eychmüller, Colloidal nanocrystal-based gels and aerogels: material aspects and application perspectives, J. Phys. Chem. Lett. 3 (2012) 8–17.
[73] S. Roy, M.S. Hegde, G. Madras, Catalysis for NOx abatement, Appl. Energy 86 (2009) 2283–2297.
[74] A. Baiker, B. Handy, J. Nickl, M. Schraml-Marth, A. Wokaun, Selective catalytic reduction of nitric oxide over vanadia grafted on titania. Influence of vanadia loading on structural and catalytic properties of catalysts, Catal. Lett. 14 (1992) 89–99.
[75] W. Shan, H. Song, Catalysts for the selective catalytic reduction of NOx with NH_3 at low temperature, Catal. Sci. Technol. 5 (2015) 4280–4290.
[76] R.J. Willey, C.-T. Wang, J.B. Peri, Vanadium–titanium oxide aerogel catalysts, J. Non-Cryst. Solids 186 (1995) 408–414.
[77] G.C. Bond, Vanadium oxide monolayer catalysts preparation, characterization and catalytic activity, Appl. Catal. 71 (1991) 1–31.
[78] Y. Watanabe, M. Imanari, M. Takeuchi, S. Matsuda, S. Uno, T. Mori, F. Nakajirna, Parametric studies of catalysts for NOx control from stationary power plants, JP 75128680 (9 October 1975).
[79] J. Leyrer, Solid–solid wetting and formation of monolayers in supported oxide systems, Surf. Sci. 201 (1988) 603–623.
[80] A. Baiker, P. Dollenmeier, M. Glinski, A. Reller, Selective catalytic reduction of nitric oxide with ammonia: I. Monolayer and multilayers of vanadia supported on titania, Appl. Catal. 35 (1987) 351–364.
[81] J. Nickl, D. Dutoit, A. Baiker, U. Scharf, A. Wokaun, Vanadia on titania prepared by vapour deposition of vanadyl alkoxide: influence of preparation variables on structure and activity for the selective ca, Appl. Catal. A: Gen. 98 (1993) 173–193.
[82] J. Engweiler, A. Baiker, Vanadia supported on titania aerogels – morphological properties and catalytic behaviour in the selective reduction of nitric-oxide by ammonia, Appl. Catal. A: Gen. 120 (1994) 187–205.
[83] C. Hoang-Van, O. Zegaoui, P. Pichat, Vanadia–titania aerogel deNOx catalysts, J. Non-Cryst. Solids 225 (1998) 157–162.
[84] G. Busca, G. Centi, L. Marchetti, F. Trifirò, Chemical and spectroscopic study of the nature of a vanadium oxide monolayer supported on a high surface-area TiO_2 anatase, Langmuir 2 (1986) 568–577.
[85] G. Busca, G. Ricchiardi, D.S.H. Sam, J.C. Volta, Spectroscopic characterization of magnesium vanadate catalysts, Part 1. Vibrational characterization of $Mg_3(VO_4)_2$, $Mg_2V_2O_7$ and MgV_2O_6 powders, J. Chem. Soc. Faraday Trans. 90 (1994) 1161–1170.
[86] G. Busca, H. Saussey, O. Saur, J.C. Lavalley, V. Lorenzelli, FT-IR characterization of the surface acidity of different TiO_2 anatase preparations, Appl. Catal. 14 (1985) 245–260.
[87] F.J.J.G. Janssen, F.M.G. Van den Kerkhof, H. Bosch, J.R.H. Ross, Mechanism of the reaction of nitric oxide, ammonia, and oxygen over vanadia catalysts 2. Isotopic transient studies with oxygen-18 and nitrogen-15, J. Phys. Chem. 91 (1987) 6633–6638.
[88] I. Giakoumelou, C. Fountzoula, C. Kordulis, S. Boghosian, Molecular structure and catalytic activity of V_2O_5/TiO_2 catalysts for the SCR of NO by NH_3: in situ Raman spectra in the presence of O_2, NH_3, NO, H_2, H_2O, and SO_2, J. Catal. 239 (2006) 1–12.
[89] M. Kang, J. Choi, Y. Tae Kim, E. Duck Park, C. Burm Shin, D.J. Suh, J. Eui Yie, Effects of preparation methods for V_2O_5–TiO_2 aerogel catalysts on the selective catalytic reduction of NO with NH_3, Korean J. Chem. Eng. 26 (2009) 884–889.
[90] M.J. Lazaro, S. Ascaso, S.P. Rodriguez, J.C. Calderon, M.E. Galvez, A.J. Nieto, R. Moliner, A. Boyano, D. Sebastian, C. Alegre, L. Calvillo, V. Celorrio, Carbon-based catalysts: synthesis and applications, C. R. Chim. 18 (2015) 1229–1241.
[91] N. Mahata, A.R. Silva, M.F.R. Pereira, C. Freire, B. Castro, J.L. Figueiredo, Anchoring of a [Mn(salen)Cl] complex onto mesoporous carbon xerogels, J. Colloid Interface Sci. 311 (2007) 152–158.
[92] A.M. ElKhatat, S.A. Al-Muhtaseb, Advances in tailoring resorcinol–formaldehyde organic and carbon gels, Adv. Mater. 23 (2011) 2887–2903.

[93] S.A. Al-Muhtaseb, J.A. Ritter, Preparation and properties of resorcinol–formaldehyde organic and carbon gels, Adv. Mater. 15 (2003) 101–114.
[94] N. Job, A. Théry, P. René, J. Marien, J.L. Kocon, J.-N. Rouzaud, F. Béguin, J.-P. Pirard, Carbon aerogels, cryogels and xerogels: influence of the drying method on the textural properties of porous carbon materials, Carbon 43 (2005) 2481–2494.
[95] L. Zubizarreta, A. Arenillas, J.-P. Pirard, J.J. Pis, N. Job, Tailoring the textural properties of activated carbon xerogels by chemical activation with KOH, Microporous Mesoporous Mater. 115 (2008) 480–490.
[96] M.E. Gálvez, M.J. Lázaro, R. Moliner, Novel activated carbon-based catalyst for the selective catalytic reduction of nitrogen oxide, Catal. Today 102–103 (2005) 142–147.
[97] H. Teng, Y.-T. Tu, Y.-C. Lai, C.-C. Lin, Reduction of NO with NH_3 over carbon catalysts: the effects of treating carbon with H_2SO_4 and HNO_3, Carbon 39 (2001) 575–582.
[98] J.P.S. Sousa, M.F.R. Pereira, J.L. Figueiredo, Carbon xerogel catalyst for NO oxidation, Catalysts 2 (2012) 447–465.
[99] K. Kaneko, Z. Wang, T. Suzuki, S. Ozeki, N. Kosugi, H. Kuroda, Micropore filling of supercritical NO on Cu-doped iron oxide dispersed activated carbon fibers, J. Colloid Interface Sci. 142 (1991) 489–496.
[100] M. Yosikawa, A. Yasutake, I. Mochida, Low-temperature selective catalytic reduction of NOx by metal oxides supported on active carbon fibers, Appl. Catal. A: Gen. 173 (1998) 239–245.
[101] G. Marbán, A.B. Fuertes, Low-temperature SCR of NOx with NH_3 over Nomex™ rejects-based activated carbon fibre composite-supported manganese oxides: part I. Effect of pre-conditioning of the carbonaceous support, Appl. Catal. B: Environ. 34 (2001) 43–53.
[102] G. Marbán, A.B. Fuertes, Low-temperature SCR of NOx with NH_3 over Nomex™ rejects-based activated carbon fibre composite-supported manganese oxides: part II. Effect of procedures for impregnation and active phase formation, Appl. Catal. B: Environ. 34 (2001) 55–71.
[103] Z. Zhu, Z. Liu, S. Liu, H. Niu, Catalytic NO reduction with ammonia at low temperatures on V_2O_5/AC catalysts: effect of metal oxides addition and SO_2, Appl. Catal. B: Environ. 30 (2001) 267–276.
[104] M.J. Lazaro, A. Boyano, M.E. Galvez, M.T. Izquierdo, E. García-Bordeje, C. Ruiz, R. Juan, R. Moliner, Novel carbon based catalysts for the reduction of NO: influence of support precursors and active phase loading, Catal. Today 137 (2008) 215–221.
[105] M.J. Lazaro, M.E. Galvez, C. Ruiz, R. Juan, R. Moliner, Vanadium loaded carbon-based catalysts for the reduction of nitric oxide, Appl. Catal. B: Environ. 68 (2006) 130–138.
[106] R.D. Vidic, C.H. Tessmer, L.J. Uranowski, Impact of surface properties of activated carbons on oxidative coupling of phenolic compounds, Carbon 35 (1997) 1349–1359.
[107] A. Berenjian, N. Chan, H.J. Malmiri, Volatile organic compounds removal methods: a review, Am. J. Biochem. Biotechnol. 8 (2012) 220–229.
[108] F. IKhan, A. Ghoshal, Removal of volatile organic compounds from polluted air, J. Loss Prev. Process Ind. 13 (2000) 527–545.
[109] E. Noordally, J.R. Richmond, S.F. Tahir, Destruction of volatile organic compounds by catalytic oxidation, Catal. Today 17 (1993) 359–366.
[110] P. Papaefthimiou, T. Ioannides, X.E. Verykios, Combustion of non-halogenated volatile organic compounds over group VIII metal catalysts, Appl. Catal. B: Environ. 13 (1997) 175–184.
[111] P.-O. Larsson, A. Andersson, Oxides of copper, ceria promoted copper, manganese and copper manganese on Al_2O_3 for the combustion of CO, ethyl acetate and ethanol, Appl. Catal. B: Environ. 24 (2000) 175–192.
[112] C.M. Pradier, F. Rodrigues, P. Marcus, M.V. Landau, M.L. Kaliya, A. Gutman, M. Herskowitz, Supported chromia catalysts for oxidation of organic compounds: the state of chromia phase and catalytic performance, Appl. Catal. B: Environ. 27 (2000) 73–85.
[113] J.J. Spivey, Complete catalytic oxidation of volatile organics, Ind. Eng. Chem. Res. 26 (1987) 2165–2180.
[114] T. García, B. Solsona, S.H. Taylor, Naphthalene total oxidation over metal oxide catalysts, Appl. Catal. B 66 (2006) 92–99.
[115] S.C. Kim, C.Y. Park, The complete oxidation of a volatile organic compound (toluene) over supported metal oxide catalysts, Res. Chem. Intermed. 28 (2002) 441–449.
[116] D. Kulkarni, I.E. Wachs, Isopropanol oxidation by pure metal oxide catalysts: number of active surface sites and turnover frequencies, Appl. Catal. A 237 (2002) 121–137.
[117] W.B. Li, W.B. Chu, M. Zhuang, J. Hua, Catalytic oxidation of toluene on Mn-containing mixed oxides prepared in reverse microemulsions, Catal. Today 93–95 (2004) 205–209.
[118] B.P. Barbero, L. Costa-Almeida, O. Sanz, M.R. Morales, L.E. Cadus, M. Montes, Wash coating of metallic monoliths with a MnCu catalyst for catalytic combustion of volatile organic compounds, Chem. Eng. J. 139 (2008) 430–435.
[119] C. Hu, Q. Zhu, Z. Jiang, Nanosized CuO–$Zr_xCe_{1-x}O_y$ aerogel catalysts prepared by ethanol supercritical drying for catalytic deep oxidation of benzene, Powder Technol. 194 (2009) 109–114.
[120] L.F. Liotta, Catalytic oxidation of volatile organic compounds on supported noble metals, Appl. Catal. B 100 (2010) 403–412.
[121] P. Papaefthimiou, T. Ioannides, X.E. Verykios, Performance of doped Pt/TiO_2 (W6+) catalysts for combustion of volatile organic compounds (VOCS), Appl. Catal. B 15 (1998) 75–92.
[122] F.J. Maldonado-Hódar, Removing aromatic and oxygenated VOCs from polluted air stream using Pt–carbon aerogels: assessment of their performance as adsorbents and combustion catalysts, J. Hazard. Mater. 194 (2011) 216–222.
[123] S. Morales-Torres, F. Carrasco-Marín, A.F. Pérez-Cadenas, F.J. Maldonado-Hódar, Coupling noble metals and carbon supports in the development of combustion catalysts for the abatement of BTX compounds in air streams, Catalysts 5 (2015) 774–799.
[124] C. Moreno-Castilla, F.J. Maldonado-Hódar, A.F. Pérez-Cadenas, Physicochemical surface properties of Fe, Co, Ni, and Cu-doped monolithic organic aerogels, Langmuir 19 (2003) 5650–5660.
[125] F. Duarte, F.J. Maldonado-Hódar, A.F. Pérez-Cadenas, L.M. Madeira, Fenton-like degradation of azo-dye Orange II catalyzed by transition metals on carbon aerogels, Appl. Catal. B: Environ. 85 (2009) 139–147.
[126] F.J. Maldonado-Hódar, C. Moreno-Castilla, A.F. Pérez-Cadenas, Catalytic combustion of toluene on platinum-containing monolithic carbon aerogels, Appl. Catal. B: Environ. 54 (2004) 217–224.
[127] S. Morales-Torres, A.F. Pérez-Cadenas, F. Kapteijn, F. Carrasco-Marín, F.J. Maldonado-Hódar, J.A. Moulijn, Palladium and platinum catalysts supported on carbon nanofiber coated monoliths for low-temperature combustion of BTX, Appl. Catal. B 89 (2009) 411–419.
[128] A. O'Malley, B.K. Hodnett, The influence of volatile organic compound structure on conditions required for total oxidation, Catal. Today 54 (1999) 31–38.
[129] S.A.C. Carabineiro, X. Chen, O. Martynyuk, N. Bogdanchikova, M. Avalos-Borja, A. Pestryakov, P.B. Tavares, J.J.M. Órfão, M.F.R. Pereira, J.L. Figueiredo, Gold supported on metal oxides for volatile organic compounds total oxidation, Catal. Today 244 (2015) 103–114.
[130] A.A. Dos Santos, K.M.N. Lima, R.T. Figueiredo, S.M.D.S. Egues, A.L.D. Ramos, Toluene deep oxidation over noble metals, copper and vanadium oxides, Catal. Lett. 114 (2007) 59–63.
[131] V.P. Santos, S.A.C. Carabineiro, P.B. Tavares, M.F.R. Pereira, J.J.M. Órfão, J.L. Figueiredo, Oxidation of CO, ethanol and toluene over TiO_2 supported noble metal catalysts, Appl. Catal. B 99 (2010) 198–205.
[132] L.S. Escandón, S. Ordóñez, A. Vega, F.V. Díez, Sulphur poisoning of palladium catalysts used for methane combustion: effect of the support, J. Hazard. Mater. 153 (2008) 742–750.
[133] D.P. Debecker, B. Farin, E.M. Gaigneaux, C. Sanchez, C. Sassoye, Total oxidation of propane with a nano-RuO_2/TiO_2 catalyst, Appl. Catal. A 481 (2014) 11–18.
[134] Y. Yazawa, N. Takagi, H. Yoshida, S.-I. Komai, A. Satsuma, T. Tanaka, S. Yoshida, T. Hattori, The support effect on propane combustion over platinum catalyst: control of the oxidation-resistance of platinum by the acid strength of support materials, Appl. Catal. A 233 (2002) 103–112.
[135] Y. Yazawa, H. Yoshida, N. Takagi, S.-I. Komai, A. Satsuma, T. Hattori, Acid strength of support materials as a factor controlling oxidation state of palladium catalyst for propane combustion, J. Catal. 187 (1999) 15–23.
[136] H. Huang, Y. Xu, Q. Fenga, D.Y.C. Leung, Low temperature catalytic oxidation of volatile organic compounds: a review, Catal. Sci. Technol. 5 (2015) 2649–2669.
[137] K.J. Kim, S.I. Boo, H.G. Ahn, Preparation and characterization of the bimetallic Pt-Au/ZnO/Al_2O_3 catalysts: influence of Pt-Au molar ratio on the catalytic activity for toluene oxidation, J. Ind. Eng. Chem. Commun. 15 (2009) 92–97.
[138] M. Haruta, Size- and support-dependency in the catalysis of gold, Catal. Today 36 (1997) 153–166.
[139] J. Choi, C.B. Shin, T.-J. Park, D.J. Suh, Characteristics of vanadia–titania aerogel catalysts for oxidative destruction of 1,2-dichlorobenzene, Appl. Catal. A: Gen. 311 (2006) 105–111.
[140] M.V. Landau, G.E. Shter, L. Titelman, V. Gelman, H. Rotter, G.S. Grader, M. Herskowitz, Alumina foam coated with nanostructured chromia aerogel: efficient catalytic material for complete combustion of chlorinated VOC, Ind. Eng. Chem. Res. 45 (2006) 7462–7469.
[141] A. Mishra, R. Prasad, A review on preferential oxidation of carbon monoxide in hydrogen rich gases, Bull. Chem. React. Eng. Catal. 6 (2011) 1–14.
[142] P.C. Hulteberg, J.G.M. Brandin, F.A. Silversand, M. Lundberg, Preferential oxidation of carbon monoxide on mounted and unmounted noble-metal catalysts in hydrogen-rich streams, Int. J. Hydrogen Energy Fuels 30 (2005) 1235–1240.
[143] Y.Y. Huang, A.A. Wang, X.X. Wang, T.T. Zhang, Preferential oxidation of CO under excess H_2 conditions over iridium catalysts, Int. J. Hydrogen Energy 32 (2007) 3880–3886.
[144] K.H. Kim, E.D. Park, H.C. Lee, D. Lee, Selective CO removal in a H_2-rich stream over supported Ru catalysts for the polymer electrolyte membrane fuel cell (PEMFC), Appl. Catal. A: Gen. 366 (2009) 363–369.
[145] M.-C. Jo, G.-H. Kwon, W. Li, A.M. Lane, Preparation and characteristics of pretreated Pt/alumina catalysts for the preferential oxidation of carbon monoxide, J. Ind. Eng. Chem. 15 (2009) 336–341.
[146] L.H. Chang, Y.L. Yeh, Y.W. Chen, Preferential oxidation of CO in hydrogen stream over nano-gold catalysts prepared by photodeposition method, Int. J. Hydrogen Energy 33 (2008) 1965–1974.
[147] E. Quinet, L. Piccolo, H. Daly, F.C. Meunier, F. Morfin, A. Valcarcel, F. Diehl, P. Avenier, V. Caps, J.-L. Rousset, H_2-induced promotion of CO oxidation over unsupported gold, Catal. Today 138 (2008) 43–49.
[148] Y.-F. Yang, P. Sangeetha, Y.-W. Chen, Au/TiO_2 catalysts prepared by photo-deposition method for selective CO oxidation in H_2 stream, Int. J. Hydrogen Energy 34 (2009) 8912–8920.

[149] F. Marino, C. Descorme, D. Duprez, Supported base metal catalysts for the preferential oxidation of carbon monoxide in the presence of excess hydrogen (PROX), Appl. Catal. B: Environ. 58 (2005) 75–183.
[150] V. Ramaswamy, S. Malwadkar, S. Chilukuri, Cu–Ce mixed oxides supported on Al-pillared clay: effect of method of preparation on catalytic activity in the preferential oxidation of carbon monoxide, Appl. Catal. B: Environ. 84 (2008) 21–29.
[151] G. Avgouropoulos, T. Ioannides, H. Matralis, Influence of the preparation method on the performance of $CuO–CeO_2$ catalysts for the selective oxidation of CO, Appl. Catal. B: Environ. 56 (2005) 87–93.
[152] J. Choi, C.B. Shin, D. Jin Suh, Co-promoted Pt catalysts supported on silica aerogel for preferential oxidation of CO, Catal. Commun. 9 (2008) 880–885.
[153] C. Kwak, T.-J. Park, D.J. Suh, Preferential oxidation of carbon monoxide in hydrogen-rich gas over platinum–cobalt–alumina aerogel catalysts, Chem. Eng. Sci. 60 (2005) 1211–1217.
[154] Y. Tai, K. Tajiri, Preparation, thermal stability, and CO oxidation activity of highly loaded Au/titania-coated silica aerogel catalysts, Appl. Catal. A: Gen. 342 (2008) 113–118.
[155] M. Haruta, When gold is not noble: catalysis by nanoparticles, Chem. Rec. 3 (2003) 75–87.
[156] J. Yang, W. Ma, D. Chen, A. Holmen, B.H. Davis, Fischer–Tropsch synthesis: a review of the effect of CO conversion on methane selectivity, Appl. Catal. A: Gen. 470 (2014) 250–260.
[157] Y.H. Hu, E. Ruckenstein, Binary MgO-based solid solution catalyst for methane conversion to syngas, Catal. Rev. 44 (2002) 423–453.
[158] B.Q. Xu, J.M. Wei, H.Y. Wang, K.Q. Sun, Q.M. Zhu, Nano-MgO: novel preparation and application as support of Ni catalyst for CO_2 reforming of methane, Catal. Today 68 (2001) 217–225.
[159] J. Zhang, H. Wang, A.K. Dalai, Development of stable bimetallic catalysts for carbon dioxide reforming of methane, J. Catal. 249 (2007) 300–310.
[160] L. De Rogatis, T. Montini, A. Cognigni, L. Olivi, P. Fornasiero, Methane partial oxidation on NiCu-based catalysts, Catal. Today 145 (2009) 176–185.
[161] S. De, J. Zhang, R. Luque, N. Yan, Ni-based bimetallic heterogeneous catalysts for energy and environmental applications, Energy Environ. Sci. 9 (2016) 3314–3347.
[162] J.-H. Kim, D.J. Suh, T.-J. Park, K.-L. Kim, Effect of metal particle size on coking during CO_2 reforming of CH_4 over Ni-alumina aerogel catalysts, Appl. Catal. A 197 (2000) 191–200.
[163] S. Therdthianwong, C. Siangchin, A. Therdthianwong, Improvement of coke resistance of Ni/Al_2O_3 catalyst in CH_4/CO_2 reforming by ZrO_2 addition, Fuel Process. Technol. 89 (2008) 160–168.
[164] H.T. Jiang, H.Q. Li, H.B. Xu, Y. Zhang, Preparation of$Ni/MgxTi_{1-x}O$ catalysts and investigation on their stability in tri-reforming of methane, Fuel Process. Technol. 88 (2007) 988–995.
[165] M.A. Goula, A.A. Lemonidou, A.M. Efstathiou, Characterization of carbonaceous species formed during reforming of CH_4 with CO_2 over $Ni/CaO–Al_2O_3$ catalysts studied by various transient techniques, J. Catal. 161 (1996) 626–640.
[166] J.-H. Kim, D.J. Suh, T.-J. Park, K.-L. Kim, Effect of metal particle size on coking during CO_2 reforming of CH_4 over Ni-alumina aerogel catalysts, Appl. Catal. A: Gen. 197 (2000) 191–200.
[167] M. Inoue, K. Sato, T. Nakamura, T. Inui, Glycothermal synthesis of zirconia-rare earth oxide solid solutions, Catal. Lett. 65 (2000) 79–83.
[168] M.C.J. Bradford, M.A. Vannice, Catalytic reforming of methane with carbon dioxide over nickel catalysts I. Catalyst characterization and activity, Appl. Catal. A 142 (1996) 73–96.
[169] J.A. Montoya, E. Romero-Pascual, C. Gimon, P. Del Angel, A. Monzón, Methane reforming with CO_2 over $Ni/ZrO_2–CeO_2$ catalysts prepared by sol–gel, Catal. Today 63 (2000) 71–85.
[170] Y.-G. Chen, K. Tomishige, K. Yokoyama, K. Fujimoto, Catalytic performance and catalyst structure of nickel–magnesia catalysts for CO_2 reforming of methane, J. Catal. 184 (1999) 479–490.
[171] L. Chen, Q. Zhu, R. Wu, Effect of Co–Ni ratio on the activity and stability of Co–Ni bimetallic aerogel catalyst for methane Oxy-CO_2 reforming, Int. J. Hydrogen Energy 36 (2011) 2128–2136.
[172] H. Li, H. Xu, J. Wang, Methane reforming with CO_2 to syngas over CeO_2-promoted $Ni/Al_2O_3–ZrO_2$ catalysts prepared via a direct sol–gel process, J. Nat. Gas Chem. 20 (2011) 1–8.
[173] T. Osaki, T. Tanaka, T. Horiuchi, T. Sugiyama, K. Suzuki, T. Mori, Application of $NiO–Al_2O_3$ aerogels to the CO_2-reforming of CH_4, Appl. Organomet. Chem. 14 (2000) 789–793.
[174] T. Osaki, T. Horiuchi, T. Sugiyama, K. Suzuki, T. Mori, Catalysis of $NiO–Al_2O_3$ aerogels for the CO_2-reforming of CH_4, Catal. Lett. 52 (1998) 171–180.
[175] Z. Hao, Q. Zhu, Z. Lei, H. Li, $CH_4–CO_2$ reforming over Ni/Al_2O_3 aerogel catalysts in a fluidized bed reactor, Powder Technol. 182 (2008) 474–479.
[176] F. Wang, J. Zhu, J.M. Beeckmans, Pressure gradient and particle adhesion in the pneumatic transport of cohesive fine powders, Int. J. Multiphase Flow 26 (2000) 245–265.
[177] X. Tao, M. Bai, X. Li, H. Long, S. Shang, Y. Yin, X. Dai, $CH_4–CO_2$ reforming by plasma – challenges and opportunities, Prog. Energy Combust. Sci. 37 (2011) 113–124.
[178] Z. Hao, Q. Zhu, Z. Jiang, H. Li, Fluidization characteristics of aerogel Co/Al_2O_3 catalyst in a magnetic fluidized bed and its application to $CH_4–CO_2$ reforming, Powder Technol. 183 (2008) 46–52.
[179] Z. Jiang, X. Liao, Y. Zhao, Comparative study of the dry reforming of methane on fluidised aerogel and xerogel $Ni–Al_2O_3$ catalysts, Appl. Petrochem. Res. 3 (2013) 91–99.
[180] Z. Xu, Y. Li, J. Zhang, L. Chang, R. Zhou, Z. Duan, Ultrafine $NiO–La_2O_3–Al_2O_3$ aerogel: a promising catalyst for CH_4/CO_2 reforming, Appl. Catal. A: Gen. 213 (2001) 65–71.
[181] Z. Hao, Q. Zhu, Z. Jiang, B. Hou, H. Li, Characterization of aerogel Ni/Al_2O_3 catalysts and investigation on their stability for $CH_4–CO_2$ reforming in a fluidized bed, Fuel Process. Technol. 90 (2009) 113–121.
[182] P. Li, J. Li, Q. Zhu, L. Cui, H. Li, Effect of granulation on the activity and stability of a $Co–Al_2O_3$ aerogel catalyst in a fluidized-bed reactor for $CH_4–CO_2$ reforming, RSC Adv. 3 (2013) 8939–8946.
[183] J.M. Coronado, A.J. Maira, J.C. Conesa, K.L. Yeung, V. Augugliaro, J. Soria, EPR study of the surface characteristics of nanostructured TiO_2 under UV irradiation, Langmuir 17 (2001) 5368–5374.
[184] D.T. Horvath, Synthesis, Characterization, and Photocatalytic Testing of Titania-Based Aerogels for the Degradation of Volatile Organic Compounds, University of Connecticut, 2012.
[185] Y.-C. Chiang, W.-Y. Cheng, S.-Y. Lu, Titania aerogels as a superior mesoporous structure for photoanodes of dye-sensitized solar cells, Int. J. Electrochem. Sci. 7 (2012) 6910–6919.
[186] G. Kovács, Z. Pap, C. Coteț, V. Coșoveanu, L. Baia, V. Danciu, Photocatalytic, morphological and structural properties of the $TiO_2–SiO_2–Ag$ porous structures based system, Materials 8 (2015) 1059–1073.
[187] M.R. Ayers, A.J. Hunt, Titanium oxide aerogels prepared from titanium metal and hydrogen peroxide, Mater. Lett. 34 (1998) 290–293.
[188] L. Baia, A. Vulpoi, T. Radu, É. Karácsonyi, A. Dombi, K. Hernádi, V. Danciu, S. Simon, K. Norén, S.E. Canton, G. Kovács, Zs. Pap, TiO_2/WO_3/Au nanoarchitectures' photocatalytic activity "from degradation intermediates to catalysts' structural peculiarities" part II: aerogel based composites-fine details by spectroscopic means, Appl. Catal. B: Environ. 148–149 (2014) 589–600.
[189] L. Brown, A. Anderson, M. Carroll, Fabrication of titania and titania–silica aerogels using rapid supercritical extraction, J. Sol–Gel Sci. Technol. 62 (2012) 404–413.
[190] R. Hutter, T. Mallat, A. Baiker, Selective epoxidation of α-isophorone with mesoporous titania–silica aerogels and tert-butyl hydroperoxide, J. Chem. Soc. Chem. Commun. (1995) 2487–2488.
[191] L. Chen, J. Zhu, Y.-M. Liu, Y. Cao, H.-X. Li, H.-Y. He, W.-L. Dai, K.-N. Fan, Photocatalytic activity of epoxide sol–gel derived titania transformed into nanocrystalline aerogel powders by supercritical drying, J. Mol. Catal. A: Chem. 255 (2006) 260–268.
[192] S.Y. Chai, Y.J. Kim, W.I. Lee, Photocatalytic WO_3/TiO_2 nanoparticles working under visible light, J. Electroceram. 17 (2006) 909–912.
[193] H. Li, S.G. Sunol, A.K. Sunol, Development of titanium-dioxide-based aerogel catalyst with tunable nanoporosity and photocatalytic activity, Nanotechnology 23 (2012) 294012–294017.
[194] S. Cao, K.L. Yeung, P.-L. Yue, Preparation of freestanding and crack-free titania–silica aerogels and their performance for gas phase, photocatalytic oxidation of VOCs, Appl. Catal. B: Environ. 68 (2006) 99–108.
[195] W.I. Kim, I.K. Hong, Synthesis of monolithic titania–silica composite aerogels with supercritical drying process, J. Ind. Eng. Chem. 9 (2003) 728–734.
[196] B. Malinowska, J. Walendziewski, D. Robert, J.V. Weber, M. Stolarski, The study of photocatalytic activities of titania and titania–silica aerogels, Appl. Catal. B: Environ. 46 (2003) 441–451.
[197] M. Schneider, A. Baiker, High-surface-area titania aerogels: preparation and structural properties, J. Mater. Chem. 2 (1992) 587–589.
[198] A.J. Maira, K.L. Yeung, C.Y. Lee, P.L. Yue, C.K. Chan, Size effects in gas-phase photo-oxidation of trichloroethylene using nanometer-sized TiO_2 catalysts, J. Catal. 192 (2000) 185–196.
[199] S. Yoda, K. Ohtake, Y. Takebayashi, T. Sugeta, T. Sako, T. Sato, Preparation of $SiO_2–TiO_2$ aerogels using supercritical impregnation, J. Sol–Gel Sci. Technol. 19 (2000) 719–723.
[200] S. Yoda, K. Ohtake, Y. Takebayashi, T. Sugeta, T. Sako, T. Sato, Preparation of titania–impregnated silica aerogels and their application to removal of benzene in air, J. Mater. Chem. 10 (2000) 2151–2156.
[201] N. Yao, S. Cao, K.L. Yeung, Mesoporous $TiO_2–SiO_2$ aerogels with hierarchal pore structures, Microporous Mesoporous Mater. 117 (2009) 570–579.
[202] Y. Boyjoo, H. Sun, J. Liu, V.K. Pareek, S. Wang, A review on photocatalysis for air treatment: from catalyst development to reactor design, Chem. Eng. J. 310 (2017) 537–559.
[203] J. Lasek, Y.-H. Yu, J.C.S. Wu, Removal of NOx by photocatalytic processes, J. Photochem. Photobiol. C: Photochem. Rev. 14 (2013) 29–52.
[204] S. Yamazoe, Y. Masutani, K. Teramura, Y. Hitomi, T. Shishido, T. Tanaka, Promotion effect of tungsten oxide on photo-assisted selective catalytic reduction of NO with NH_3 over TiO_2, Appl. Catal. B: Environ. 83 (2008) 123–130.
[205] S. Yamazoe, Y. Masutani, T. Shishido, T. Tanaka, Metal oxide promoted TiO_2 catalysts for photo-assisted selective catalytic reduction of NO with NH_3, Res. Chem. Intermed. 34 (2008) 487–494.
[206] M. Polat, A.M. Soylu, D.A. Erdogan, H. Erguven, E.I. Vovk, E. Ozensoy, Influence of the sol–gel preparation method on the photocatalytic NO oxidation performance of TiO_2/Al_2O_3 binary oxides, Catal. Today 241 (2015) 25–32.

[207] A.M. Soylu, M. Polat, D.A. Erdogan, Z. Say, C. Yıldırım, Ö. Birer, E. Ozensoy, TiO_2–Al_2O_3 binary mixed oxide surfaces for photocatalytic NOx abatement, Appl. Surf. Sci. 318 (2014) 142–149.
[208] S.J. Kim, P. Raut, S.C. Jana, G. Chase, Electrostatically active polymer hybrid aerogels for airborne nanoparticle filtration, ACS Appl. Mater. Interfaces 9 (2017) 6401–6410.
[209] M. Kampa, E. Castanas, Human health effects of air pollution, Environ. Pollut. 151 (2008) 362–367.
[210] S.J. Kim, G. Chase, S.C. Jana, The role of mesopores in achieving high efficiency airborne nanoparticle filtration using aerogel monoliths, Sep. Purif. Technol. 166 (2016) 48–54.
[211] S.J. Kim, G. Chase, S.C. Jana, Polymer aerogels for efficient removal of airborne nanoparticles, Sep. Purif. Technol. 156 (2015) 803–808.
[212] M.S. Ahmed, Y.A. Attia, Multi-metal oxide aerogel for capture of pollution gases from air, Appl. Therm. Eng. 18 (1998) 787–797.
[213] M.T. Guise, B. Hosticka, B.C. Earp, P.M. Norris, An experimental investigation of aerosol collection utilizing packed beds of silica aerogel microsphere, J. Non-Cryst. Solids 285 (2001) 317–322.
[214] A. Vohra, D.Y. Goswami, D.A. Deshpande, S.S. Block, Enhanced photocatalytic disinfection of indoor air, Appl. Catal. B: Environ. 64 (2006) 57–65.
[215] Y. Kikuchi, K. Sunada, T. Iyoda, K. Hashimoto, A. Fujishima, Inactivation of microorganisms on the photocatalytic surfaces in air, J. Photochem. Photobiol. A 106 (1997) 51–56.
[216] K. Sunada, T. Watanabe, K. Hashimoto, Antibacterial activity of TiO_2/Ti composite photocatalyst films treated by ultrasonic cleaning, J. Photochem. Photobiol. A 156 (2003) 227–233.
[217] S. Cao, Preparation, Characterization and Applications of Monolithic Titania–Silica Aerogels, School of Engineering, University of Science and Technology, Hong Kong, 2007.
[218] B. Krishnakumar, M. Swaminathan, Influence of operational parameters on photocatalytic degradation of a genotoxic azo dye Acid Violet 7 in aqueous ZnO suspensions, Spectrochim. Acta A: Mol. Biomol. Spectrosc. 81 (2011) 739–744.
[219] M. Antonopoulou, E. Evgenidou, D. Lambropoulou, I. Konstantinou, A review on advanced oxidation processes for the removal of taste and odor compounds from aqueous media, Water Res. 5 (3) (2014) 215–234.
[220] A. Asghar, A.A. Abdul Raman, W.M.A.W. Daud, Advanced oxidation processes for in-situ production of hydrogen peroxide/hydroxyl radical for textile wastewater treatment: a review, J. Clean. Prod. 87 (2015) 826–838.
[221] M.N. Chong, A.K. Sharma, S. Burn, C.P. Saint, Feasibility study on the application of advanced oxidation technologies for decentralised wastewater treatment, J. Clean. Prod. 35 (2012) 230–238.
[222] J. Fernandez, J. Bandara, A. Lopez, P. Buffat, J. Kiwi, Photoassisted Fenton degradation of nonbiodegradable azo dye (Orange II) in Fe-free solutions mediated by cation transfer membranes, Langmuir 15 (1999) 185–192.
[223] J.J. Pignatello, E. Oliveros, A. MacKay, Advanced oxidation processes for organic contaminant destruction based on the Fenton reaction and related chemistry, Crit. Rev. Environ. Sci. Technol. 36 (2006) 1–84.
[224] A.L.-T. Pham, C. Lee, F.M. Doyle, D.L. Sedlak, A silica-supported iron oxide catalyst capable of activating hydrogen peroxide at neutral pH values, Environ. Sci. Technol. 43 (2009) 8930–8935.
[225] E.G. Garrido-Ramirez, B.K.G. Theng, M.L. Mora, Clays and oxide minerals as catalysts and nanocatalysts in Fenton-like reactions – a review, Appl. Clay Sci. 47 (2010) 182–192.
[226] H. Lim, J. Lee, S. Jin, J. Kim, J. Yoon, T. Hyeon, Highly active heterogeneous Fenton catalyst using iron oxide nanoparticles immobilized in alumina coated mesoporous silica, Chem. Commun. 4 (2006) 463–465.
[227] A. Santos, P. Yustos, S. Rodríguez, F. Garcia-Ochoa, M. de Gracia, Decolorization of textile dyes by wet oxidation using activated carbon as catalyst, Ind. Eng. Chem. Res. 46 (2007) 2423–2430.
[228] J. Herney-Ramirez, M.A. Vicente, L.M. Madeirac, Heterogeneous photo-Fenton oxidation with pillared clay-based catalysts for wastewater treatment: a review, Appl. Catal. B: Environ. 98 (2010) 10–26.
[229] R. Gonzalez-Olmos, M.J. Martin, A. Georgi, F.-D. Kopinke, I. Oller, S. Malat, Fe-zeolites as heterogeneous catalysts in solar Fenton-like reactions at neutral pH, Appl. Catal. B: Environ. 125 (2012) 51–58.
[230] Y. Li, F. Hung, L.J. Hope-Weeks, W. Yan, Fe/Al binary oxide aerogels and xerogels for catalytic oxidation of aqueous contaminants, Sep. Purif. Technol. 156 (2015) 1035–1040.
[231] J.H. Ramirez, F.J. Maldonado-Hodar, A.F. Pérez-Cadenas, C. Moreno-Castilla, C.A. Costa, L.M. Madeira, Azo-dye Orange II degradation by heterogeneous Fenton-like reaction using carbon-Fe catalysts, Appl. Catal. B: Environ. 75 (2007) 312–323.
[232] Y. Hardjono, H. Sun, H. Tian, C.E. Buckley, S. Wang, Synthesis of Co oxide doped carbon aerogel catalyst and catalytic performance in heterogeneous oxidation of phenol in water, Chem. Eng. J. 174 (2011) 376–382.
[233] N.K. Daud, M.A. Ahmad, B.H. Hameed, Decolorization of Acid Red 1 dye solution by Fenton-like process using Fe–Montmorillonite K10 catalyst, Chem. Eng. J. 165 (2010) 111–116.
[234] M.T. Amin, A.A. Alazba, U. Manzoor, A review of removal of pollutants from water/wastewater using different types of nanomaterials, Adv. Mater. Sci. Eng. 2014 (2014) 1–24.
[235] M. Sanchez-Polo, J. Rivera-Utrilla, U. von Gunten, Metal-doped carbon aerogels as catalysts during ozonation processes in aqueous solutions, Water Res. 40 (2006) 3375–3384.
[236] E. Hu, X. Wu, S. Shang, X.-M. Tao, S.-X. Jiang, L. Gan, Catalytic ozonation of simulated textile dyeing wastewater using mesoporous carbon aerogel supported copper oxide catalyst, J. Clean. Prod. 112 (2016) 4710–4718.
[237] X. Huang, C. Tan, Z. Yin, H. Zhang, 25th anniversary article: hybrid nanostructures based on two-dimensional nanomaterials, Adv. Mater. 26 (2014) 2185–2204.
[238] S. Cao, K.L. Yeung, P.-L. Yue, An investigation of trichloroethylene photocatalytic oxidation on mesoporous titania–silica aerogel catalysts, Appl. Catal. B: Environ. 76 (2007) 64–72.
[239] S. Cao, K.L. Yeung, J.K.C. Kwan, P.M.T. To, S.C.T. Yu, An investigation of the performance of catalytic aerogel filters, Appl. Catal. B: Environ. 86 (2009) 127–136.
[240] W. Liu, J. Cai, Z. Li, Self-assembly of semiconductor nanoparticles/reduced graphene oxide (RGO) composite aerogels for enhanced photocatalytic performance and facile recycling in aqueous photocatalysis, ACS Sustain. Chem. Eng. 3 (2015) 277–282.
[241] X. Shao, W. Lu, R. Zhang, F. Pan, Enhanced photocatalytic activity of TiO_2-C hybrid aerogels for methylene blue degradation, Sci. Rep. 3 (2013) 3018.
[242] F. Orellana-García, M.A. Álvarez, M. Victoria López-Ramón, J. Rivera-Utrilla, M. Sánchez-Polo, M.Á. Fontecha-Cámara, Photoactivity of organic xerogels and aerogels in the photodegradation of herbicides from waters, Appl. Catal. B: Environ. 181 (2016) 94–102.
[243] J. Cai, W. Liu, Z. Li, One-pot self-assembly of Cu_2O/RGO composite aerogel for aqueous photocatalysis, Appl. Surf. Sci. 358 (2015) 146–151.
[244] X. Li, S. Yang, J. Sun, P. He, X. Xu, G. Ding, Tungsten oxide nanowire-reduced graphene oxide aerogel for high-efficiency visible light photocatalysis, Carbon 78 (2014) 38–48.
[245] Y. Jin, M. Wu, G. Zhao, M. Li, Photocatalysis-enhanced electrosorption process for degradation of high-concentration dye wastewater on TiO_2/carbon aerogel, Chem. Eng. J. 168 (2011) 1248–1255.
[246] D. Bamba, M. Coulibaly, C.I. Fort, C.L. CoteSt, Z. Pap, K. Vajda, E.G. Zoro, N. Alfred Yao, V. Danciu, D. Robert, Synthesis and characterization of TiO_2/C nanomaterials: applications in water treatment, Phys. Status Solidi B 252 (2015) 2503–2511.
[247] M. Miao, G. Wang, S. Cao, X. Feng, J. Fang, L. Shi, TEMPO-mediated oxidized winter melon-based carbonaceous aerogel as an ultralight 3D support for enhanced photodegradation of organic pollutants, Phys. Chem. Chem. Phys. 17 (2015) 24901–24907.
[248] Z. Zhou, X. Zhang, C. Lu, L. Lan, G. Yuan, Polyaniline-decorated cellulose aerogel nanocomposite with strong interfacial adhesion and enhanced photocatalytic activity, RSC Adv. 4 (2014) 8966–8972.
[249] S.K. Papageorgiou, F.K. Katsaros, E.P. Favvas, G.E. Romanos, C.P. Athanasekou, K.G. Beltsios, O.I. Tzialla, P. Falaras, Alginate fibers as photocatalyst immobilizing agents applied in hybrid photocatalytic/ultrafiltration water treatment processes, Water Res. 46 (2012) 1858–1872.
[250] M. Shi, W. Wei, Z. Jiang, H. Han, J. Gao, J. Xie, Biomass-derived multifunctional TiO_2/carbonaceous aerogel composite for the highly efficient photocatalyst, RSC Adv. 6 (2016) 25255–25266.
[251] H.S. Kibombo, A.S. Weber, C.-M. Wu, K.R. Raghupathi, R.T. Koodalia, Effectively dispersed europium oxide dopants in TiO_2 aerogel supports for enhanced photocatalytic pollutant degradation, J. Photochem. Photobiol. A: Chem. 269 (2013) 49–58.
[252] Z. Pap, A. Radu, I.J. Hidi, G. Melinte, L. Diamandescu, T. Popescu, L. Baia, V. Danciu, M. Baia, Behavior of gold nanoparticles in a titania aerogel matrix: photocatalytic activity assessment and structure investigations, Chin. J. Catal. 34 (2013) 734–740.
[253] J. Puskelova, L. Baia, A. Vulpoi, M. Baia, M. Antoniadou, V. Dracopoulos, E. Stathatos, K. Gabor, Z. Pap, V. Danciuf, P. Lianos, Photocatalytic hydrogen production using TiO_2–Pt aerogels, Chem. Eng. J. 242 (2014) 96–101.
[254] Y. Yu, M. Zhu, W. Liang, S. Rhodes, J. Fang, Synthesis of silica–titania composite aerogel beads for the removal of Rhodamine B in water, RSC Adv. 5 (2015) 72437–72443.
[255] M.S. Ahmed, Y.A. Attia, Aerogel materials for photocatalytic detoxification of cyanide wastes in water, J. Non-Cryst. Solids 186 (1995) 402–407.
[256] Z. Deng, J. Wang, Y. Zhang, Z. Weng, Z. Zhang, B. Zhou, J. Shen, L. Cheng, Preparation and photocatalytic activity of TiO_2–SiO_2 binary aerogels, Nanostruct. Mater. 11 (1999) 1313–1318.
[257] X. Gao, I.E. Wachs, Titania–silica as catalysts: molecular structural characteristics and physico-chemical properties, Catal. Today 51 (1999) 233–254.
[258] J. Zhu, J. Xiea, X. Lüa, D. Jianga, Synthesis and characterization of superhydrophobic silica and silica/titania aerogels by sol–gel method at ambient pressure, Colloids Surf. A: Physicochem. Eng. Aspects 342 (2009) 97–101.
[259] G. Zu, J. Shen, W. Wang, L. Zou, Y. Lian, Z. Zhang, Silica–titania composite aerogel photocatalysts by chemical liquid deposition of titania onto nanoporous silica scaffolds, ACS Appl. Mater. Interfaces 7 (2015) 5400–5409.
[260] A.A. Ismail, I.A. Ibrahim, Impact of supercritical drying and heat treatment on physical properties of titania/silica aerogel monolithic and its applications, Appl. Catal. A: Gen. 346 (2008) 200–205.
[261] P. Serp, J.L. Figueiredo, J.L. Faria, W. Wang, Carbon materials in photocatalysis, in: P. Serp, J.L. Figueiredo (Eds.), Carbon Materials for Catalysis, John Wiley Sons Inc., 2008.
[262] S. Sakthivel, H. Kisch, Daylight photocatalysis by carbon-modified titanium dioxide, Angew. Chem. Int. Ed. 42 (2003) 4908–4911.

[263] M. Toyoda, T. Yano, B. Tryba, S. Mozia, T. Tsumura, M. Inagaki, Preparation of carbon-coated Magneli phases TinO2$n-1$ and their photocatalytic activity under visible light, Appl. Catal. B: Environ. 88 (2009) 160–164.
[264] K. Woan, G. Pyrgiotakis, W.S. Sigmund, Photocatalytic carbon nanotube-TiO_2 composite, Adv. Mater. 21 (2009) 2233–2239.
[265] M. Liu, L. Gan, Y. Pang, Z. Xu, Z. Hao, L. Chen, Synthesis of titania–silica aerogel-like microspheres by a water-in-oil emulsion method via ambient pressure drying and their photocatalytic properties, Colloids Surf. A: Physicochem. Eng. Aspects 317 (2008) 490–495.
[266] Y.N. Kim, G.N. Shao, S.J. Jeon, S.M. Imran, P.B. Sarawade, H.T. Kim, Sol–gel synthesis of sodium silicate and titanium oxychloride based TiO_2–SiO_2 aerogels and their photocatalytic property under UV irradiation, Chem. Eng. J. 231 (2013) 502–511.
[267] L. Luo, A.T. Cooper, M. Fan, Preparation and application of nanoglued binary titania–silica aerogel, J. Hazard. Mater. 161 (2009) 175–182.
[268] C. Fan, Q.L. n, T. Ma, J. Shen, Y. Yang, H. Tang, Y. Wang, J. Yang, Fabrication of 3D $CeVO_4$/graphene aerogels with efficient visible-light photocatalytic activity, Ceram. Int. 42 (2016) 10487–10492.
[269] T.-Y. Wei, C.-Y. Kuo, Y.-J. Hsu, S.-Y. Lu, Y.-C. Chang, Tin oxide nanocrystals embedded in silica aerogel: photoluminescence and photocatalysis, Microporous Mesoporous Mater. 112 (2008) 580–588.
[270] V. Vaiano, O. Sacco, D. Sannino, P. Ciambelli, S. Longo, V. Venditto, G. Guerra, N-doped TiO_2/s-PS aerogels for photocatalytic degradation of organic dyes in wastewater under visible light irradiation, J. Chem. Technol. Biotechnol. 89 (2014) 1175–1181.